

τ -jet separation in ATLAS detector

Donatella Cavalli and Silvia Resconi

Physics Department, Milano University and INFN
I-20133 Milano, via Celoria 16, Italy

Abstract

This note documents the work done to study the τ -jets separation in ATLAS using a full simulation of the detector.

The criteria used to separate τ 's from jets are based on information both from the calorimeters and from the inner detector. The τ -identification results strongly p_T -dependent and it also depends on the η position and on the underlying event.

A τ -identification with an acceptance around 20% and a very good rejection against the jets from backgrounds (from ~ 170 to ~ 1700) can be achieved, that is essential for $A^0 \rightarrow \tau\tau$ analysis; higher acceptances for τ 's are obtained with lower jet-rejections.

The results obtained at low luminosity are not sensibly worsened going to high luminosity.

1 Introduction

Large samples of full simulated events were produced for the preparation of the ATLAS Technical Proposal (TP) [1] and the ATLAS Calorimeter Performance Technical Design Report (TDR) [2], with the aim of studying in a realistic way the performances of the ATLAS detector in the reconstruction of quantities used in the physics event analysis.

In particular a systematic study of τ -identification was performed, based on fully simulated events with a pseudoscalar Higgs A^0 decaying $\rightarrow \tau\tau$, where one of the τ -leptons decays to hadrons and the other one to lepton, and on fully simulated events containing jets. A good sensitivity to $A^0 \rightarrow \tau\tau$ channel depends crucially on the quality of the τ -identification in the ATLAS detector, since backgrounds from jets are potentially very large [1], [2], [3].

This note is organised as follows. Section 2 describes the samples of full simulated events and the detector layouts used; in section 3 it is discussed how a τ -jet is chosen in the physics complete events and how precisely the τ -jet is measured. The fourth section gives the quantities used to separate τ 's from jets. Section 5 describes the criteria used to reach the τ -identification versus jet-rejection needed for the study of the $A^0 \rightarrow \tau\tau$ channel and the sixth one gives the impact of τ -identification and jet-rejection and also of τ measurement on physics. Section 7 gives the relative dependence between τ -identification and jet-rejection as functions of p_T and η of clusters; the effect of the underlying event is shown in section 8 and the effects of cracks are described in section 9. Section 10 gives criteria for τ -veto and finally section 11 shows a comparison between τ -identification performances at low and high luminosity.

2 Event samples and detector layouts

The study of τ 's has been performed using the $A^0 \rightarrow \tau\tau$ full simulated events for A^0 masses in the range 100-500 GeV, the background events full simulated for the study of that channel and also the large jet-sample full simulated in 1997 [4]. Also a small sample of isolated τ 's has been studied.

In the following sections we call 'TPsample' the sample of events full simulated for the TP, using an old and simplified detector layout, with the electromagnetic calorimeter simulated with a parallel plate geometry and a separated preshower with two views in front of the electromagnetic calorimeter. This simplified layout is not expected to bias significantly the results.

The total 'TPsample' is of ~ 13000 signal full simulated events for 8 different A^0 masses and ~ 8000 background events ($t\bar{t}$, $b\bar{b}$, W+jets), in which ~ 10000 τ 's and ~ 10000 jets with $E_T > 40\text{GeV}$ and $|\eta| < 2.5$ respectively are present. Details can be found in Table 1 of [3].

A second sample of full simulated events ('97sample') was produced for the preparation of the calorimeter TDR and in 1997 in view of the physics TDR; it is obtained with the 'final' detailed 'Accordeon' geometry for the electromagnetic calorimeters. Details on '97sample' are reported in Tab. 1; it consists of:

- τ -jets from two samples of $A^0 \rightarrow \tau\tau$ signal: associated bbA^0 , which is the dominant A^0 production process at high $tg(\beta)$ values, and single A^0 productions ($m_A=100, 150, 300$ and 450 GeV). A total of ~ 2700 ($+3600$) τ 's with $E_T > 30$ GeV and $|\eta| < 2.5$ have been used.
- jets from typical $A^0 \rightarrow \tau\tau$ backgrounds like $t\bar{t}$, $b\bar{b}$, W+jets, in total ~ 3500 jets and ~ 600 b-jets with $E_T > 30$ GeV and $|\eta| < 2.5$.

We have also used a sample of ~ 26000 jets from the large 1997 jet-sample production, called 'jets97' in the following, consisting in light and heavy quark jets and also gluon jets from many processes (see [4]).

Finally we have also used, for some checks, a sample of 1000 full simulated isolated τ 's decaying to hadrons, at fixed $p_{T\tau}=60$ GeV and fixed $\eta_\tau=0.3$, called 'single τ '.

The results and the figures of this note are generally done using events from '97sample' and from 'jets97'; the results and the figures for 'TPsample' events were given previously in [1], [2] and [3]; however many comparisons between the different event samples are here done.

3 τ -jet choice and measurement

In all our studies (apart the studies done for cracks) τ 's from complete physics events (not isolated τ 's!) have been used, so it has to be taken into account that our results are surely worse than the results that can be obtained with single τ 's, but they are more realistic to be used for the physics analysis.

In a complete event a jet is labelled as a τ -jet if the distance of its barycenter position from the position of the hadronic decay part of the τ computed at particle level ($\vec{h}_\tau = \vec{\tau} - \vec{\nu}_\tau$) is $\Delta R = \sqrt{(\eta_{\tau\text{-jet}} - \eta_{h\tau})^2 + (\phi_{\tau\text{-jet}} - \phi_{h\tau})^2} < 0.3$. Applying

that criterium, we find that in our physics events, if $p_T(h_\tau) > 30$ GeV, in 98% of the cases we have at least 1 jet with $p_T > 30$ GeV labelled as τ -jet.

The τ -jet energy is reconstructed from the calorimeter cell energies, applying the same calibration constants used for jet reconstruction (see [2] and [3]). Fig. 1 gives the distributions of $p_T(\tau\text{-jet})$ and $p_T(h_\tau)$ and their ratio. It can be seen that the τ -jet energy is overestimated by $\sim 5\%$ because the electromagnetic content in a τ -jet is higher than in a normal jet; the cases in which the $p_T(\tau\text{-jet})/p_T(h_\tau)$ ratio is very high are due to superposition of other jets to the true τ -jet with a consequent too high reconstructed energy. Choosing only $p_T(h_\tau) > 70$ GeV gives a better ratio value with less overflow events. The resolution of the τ energy and direction measurement is given in Fig. 2. From the ΔR distribution it seems that choosing a $\Delta R < 0.1$ cut for τ -labelling would not decrease too much the efficiency: that cut could also avoid to accept some of the τ 's superposed on other jets.

In any case it will be shown in the section about the impact on physics that the precision of the τ -jet energy measurement is not so critical, because the precision of the A^0 reconstructed mass is dominated by the p_T^{miss} resolution (see [3] for all details).

4 Definition of physical quantities used for τ -jet separation

τ 's and jets are separated using both information from the calorimeters and from the inner detector.

The quantities used are:

- R_{em} that is the jet radius computed using only the electromagnetic cells contained in the jet. It is defined by the following formula:

$$\frac{\sum_{i=1}^n E_{Ti} \sqrt{(\eta_i - \eta_{cluster})^2 + (\phi_i - \phi_{cluster})^2}}{\sum_{i=1}^n E_{Ti}}$$

where i is running on all the cells in the electromagnetic calorimeters contained in a cone of $R=0.7$ around the barycenter of the cluster, whose coordinates are $(\eta_{cluster}, \phi_{cluster})$

- ΔE_T^{12} that is the fraction of transverse energy (computed both from electromagnetic and hadronic calorimeter) contained between the cones of size $R=0.2$ and 0.1 around the barycenter of the cluster;
- N_{tr} that is the number of charged tracks with p_T above a fixed cutoff (1, 2 and 5 GeV have been used) pointing to the cluster (within $\Delta R=0.3$).

Information from the first layer of the electromagnetic calorimeter, ' η strips' layer, have also been studied for events from '97sample':

- N_{strip} that is the number of hit η strips in the ' η strips' layer in the electromagnetic calorimeter

- η -width in ' η -strips' layer defined as:

$$\frac{\sqrt{\sum_{i=1}^n E_{Ti} (\eta_i - \eta_{cluster})^2}}{\sum_{i=1}^n E_{Ti}}$$

where i is running on all the cells in the first electromagnetic calorimeter layer

- $distri$ that is the distance between η of the maximum associated p_T track and η of the barycenter of the cluster in the η -strip layer.

The distributions of these quantities for the τ 's from bbA^0 events in '97sample' and for the jets from 'jets97' are very different if compared before any cut. They are shown

in Fig. 3, 4, 5, 6. These quantities are strongly correlated, so, as it will be shown after, it is not necessary to apply analysis cutoffs on all of them.

The R_{em} , ΔE_T^{12} and N_{tr} distributions are in good agreement with the distributions obtained from 'TPsample' and shown in Fig. 4.18 of [2]. Fig. 7 and 8 compare the 'TPsample' (where $p_T > 40$ GeV) to '97sample' distributions normalised to the same number of events.

As it will be shown after, there is a strong dependence of the variables we have defined above on the p_T of the cluster, so we have tried to compare 'TPsample' and '97sample' in p_T ranges as much as possible similar; for that reason only jets with $p_T > 40$ GeV were here used also for '97sample'; for the τ 's in '97sample' $p_T > 30$ GeV was used, to have the average values of p_T distributions as much as possible similar. It can be noted that R_{em} and ΔE_T^{12} are narrower for '97sample' events: that can be due to the ' η -strips' layer that gives a more accurate estimation of the variables.

On the contrary, N_{tr} is larger for '97sample' events: that can be due in part to the multiple interactions that were switched off in 'TPsample' simulations and also to the γ conversions in the material in front of the calorimeter (see Fig. 9 where the number of associated tracks with $p_T > 2$ GeV is given with and without the tracks from γ conversion). In fact the number of associated charged tracks with $p_T > 2$ GeV is sensibly higher than the number of charged particles coming from the hadronic τ decay as it can be seen from Fig. 10. Anyway it has been shown that it is possible to identify with a good efficiency the converted photons in the Inner Detector [5], so a correction for this effect is foreseen in future.

5 τ -jet separation criteria for $A^0 \rightarrow \tau\tau$ study

For the study of the $A^0 \rightarrow \tau\tau$ channel and to discard as much as possible the background events, very stringent τ -identification criteria were chosen.

A hadronic jet with $E_T > 30$ GeV and $|\eta| < 2.5$ was identified as a τ -jet if it satisfied the following criteria:

- $R_{em} < 0.07$,
- $\Delta E_T^{12} < 0.1$,
- $N_{tr} = 1$ or • $N_{tr} = 1$ or 3.

The three above cuts are strongly correlated as it can be seen from Fig. 11 and 12. Table 2 shows the efficiencies of these criteria, computed sequentially, for τ jets from single and associated $bbA^0 \rightarrow \tau\tau$ production events ('97sample'), for jets from the 'jets97' production and from the jets contained in typical backgrounds of $A^0 \rightarrow \tau\tau$ channel, which are $b\bar{b}$, $t\bar{t}$ and W +jets events.

Table 3 contains the results obtained from 'TPsample', already given in [1], [2], [3] and reported here for comparison (there is a little discrepancy with the results reported in the past because also events with $m_A = 100$ GeV are here used).

In Fig. 11 and 12 the quantities N_{strip} , η -width and $distri$ are represented after the three cuts set above. A further cut on these quantities gives no significant gain on the τ -efficiency/jet-rejection. This is due to the strong correlation of these quantities with the other ones already used, so, after the cuts, their distributions look very similar for τ 's and jets, but it must also be underlined that the cone size used in this analysis

($R=0.7$) is too large to profit in the best way from the high granularity of the η -strips. In fact the distributions of quantities from η -strips for τ 's shown in Fig. 5 have large average values and also long tails due to the fact that many low-energy particles in the event hit the η -strips within the large cone chosen. Average values are smaller and tails are not present if isolated single τ 's are studied (see Fig. 24).

An optimisation of the cone size is foreseen in future for the best use of the η -strips for τ -identification.

The pure calorimeter cuts ($R_{em} + \Delta E_T^{12}$) provide a rejection of ~ 170 against jets (from 'jets97') with an efficiency of 40% for hadronic τ -decays. Comparing with the results in Tab. 1 of [3], it can be seen that in '97sample' we have the same jet rejection with a higher τ efficiency, due to the narrower R_{em} and ΔE_T^{12} distributions, as described at the end of the previous section.

Stronger jet-rejection is achieved using also the number of associated tracks with $p_T > 2$ GeV. The ATLAS inner detector will be able (see section 3.8.5.2 of TP) to reconstruct all tracks starting from a $p_T=1$ GeV within a low-multiplicity jet environment with very high efficiency and negligible fake track rate, even at the highest luminosities expected at LHC.

The request to have only 1 associated track with $p_T > 2$ GeV reduces strongly the τ efficiency (a big effect ($\sim 20\%$) is due to the γ conversions in the material in front of the calorimeter, as it has been shown in section 4), but it provides an extra rejection factor of $\sim 3 - 9$ against jets. The request of having 1 or 3 associated tracks improves of a factor ~ 1.5 the τ acceptance, but it does not really improve the sensitivity because also \sqrt{B} , where B indicates the jet background, increases by a factor around 1.5.

Note that here the tracks from KINE bank are used: using the reconstructed tracks in the inner detector (a test has been done on a small A^0 event statistics) gives $\sim 10\%$ more of τ 's with 1 associated tracks, due to some inefficiency in tracks reconstruction. In Fig. 13 the comparison between reconstructed and KINE tracks is shown, also separately for 1-charged-prong and 3-charged-prong τ 's (note that, as it has already said at the end of previous section, the number of associated tracks to 1-charged-prong τ 's is in some cases > 1 , due to the underlying event and to the γ -conversions). From the last plot of Fig. 13 it can be seen that for 1-charged-prong τ 's in the 87% of cases the maximum p_T reconstructed track is within ± 5 GeV the maximum p_T KINE track.

The effect of changing the p_T threshold for tracks has also been studied: results are not sensibly different using 1, 2 or 5 GeV thresholds, as it can be seen from Table 2.

It is important to point out that Table 2 gives results integrated on all clusters with $p_T > 30$ GeV and $|\eta| < 2.5$ found in signal and background events (p_T distributions are given in Fig. 14 for the different jet types; p_T distribution for τ 's was already given in Fig. 1) while for a fixed set of cuts the τ -identification efficiency and the corresponding jet-rejection depend on p_T and η position of clusters (see section 7).

In our A^0 analysis, the rejection against jets from $t\bar{t}$ is better than against jets from W+jets, due to the different jet type (quark or gluon jets) and also to the different p_T distributions. Combining the τ -identification efficiencies of $t\bar{t}$ and W+jets (the relative numbers of events are similar in the samples TP and 97) we obtain a total efficiency of 0.23% which is comparable with the value 0.25% reported in Tab. 3.

The b-jet rejection is stronger than the rejection of other jets, also if it is computed with a large error: 0 b-jets survive over ~ 1600 (considering 622 b-jets in $b\bar{b}$ events and 1013 b-jets in bbA events), so we quote a b-jet rejection < 0.06 ($=1./1600$).

Fig.15 shows the τ -identification efficiency and the jet-rejection vs p_T for p_T 's between 15-130 GeV, applying the cuts described before. It can be noted that τ -identification efficiency, once fixed the cuts, increases with increasing p_T ; the jet-rejection is smoothly p_T dependent starting from 20 GeV while at low p_T it increases rapidly.

6 Impact on physics

Three mass points $m(A^0)=150, 300, 450$ GeV are here considered to explain the importance of τ -identification in the $A^0 \rightarrow \tau\tau$ analysis. The statistics used is reported in Tab.1.

To take into account also the bbA^0 production process, which is dominant for high $m(A^0)$ and high $tg(\beta)$ values, a new combined analysis has been developed: it consists in two different analyses that are performed both on single and associated A^0 production events. The first one ('a1') is the old analysis (described in [3]) with the further request to have no b-jets tagged in the event ; the second one ('a2') selects the events with the following requests:

- one b-jet tagged (againsts Z^0 and W+jets backgrounds).
- $N^0(no\ b - jets) < 3$ (against $t\bar{t}$ background).
- old analysis cuts (kinematic and τ -identification criteria) [3] except the $\Delta\phi(jet - \mu)$ cut.

Due to the opposite request to have or not to have a b-jet tagged, the two analyses are not correlated, so they are separately applied to background events and to both signal samples (single and associated A^0) and then combined.

More details about this new combined analysis will be reported in a note in preparation ([6]). Here it is interesting to compare the combined significance values obtained applying or not applying the τ identification criteria to our sets of full simulated signal and background events.

In Table 4 the expected numbers of events for signal (single and associated A^0 production) and backgrounds for an integrated luminosity of $3 * 10^4 pb^{-1}$ are given applying only the kinematic cuts from 'a2' and 'a1' analysis for the three mass points assuming $tg(\beta)=10$; the significance obtained combining the two analyses is also reported in the same Table.

In Table 5 the expected numbers of events for signal and backgrounds after kinematic plus τ -identification cuts from 'a2' and 'a1' analysis are reported, also the combined significance and the 5σ limit on $tg(\beta)$ are calculated.

Considering for example $m(A^0)=150$ GeV, at an integrated luminosity of $3 * 10^4 pb^{-1}$ and $tg(\beta)=10$, after all the kinematics cuts (see Table 4) ~ 335 signal events (summing single and associated A^0 productions) and $\sim 9 * 10^3$ background events are expected from the 'a2' analysis while from the 'a1' one ~ 711 signal events and $\sim 3 * 10^5$ background events are expected. The combined significance obtained in this case is only ~ 2 and it is even worse for higher A^0 masses (see Table 4), so without τ -identification criteria the $A^0 \rightarrow \tau\tau$ analysis is completely hopeless.

After the application of the τ -identification criteria with $N_{tr}=1$ (see Table 5), for $m_A=150$ GeV, ~ 88 signal events and ~ 57 background events are expected from the 'a2' analysis while ~ 111 signal events and ~ 1314 background events are expected from the 'a1' one.

The combined significance obtained applying the τ -identification criteria is 12.3 which is much higher than the requested significance of 5 which indeed can be obtained with a $tg(\beta)$ of 6.5.

Asking for $N_{tr}=1$ or 3 in the τ -identification criteria, the combined significance obtained is comparable or even worse with respect to the one obtained asking for $N_{tr}=1$ (see Table 5): this is due to the fact that together with the increase in the expected signal events, there is also an increase in the number of expected background events.

It has been said in section 3 that the precision of the τ -jet energy measurement is not so critical in A^0 study. In fact the biggest contributions to the width of the reconstructed invariant mass of the τ -pair are due to the assumption on the directions of the τ -decay products and to the p_T^{miss} resolution (direction and module). Using the reconstructed τ -jets instead of the τ hadronic part at particle level (h_τ) the RMS of the reconstructed mass distribution increases only by about 3% and does not change at all its central value (for many details and figures see [3]).

7 Jet-rejection vs τ -identification

Jet-rejection vs τ -identification efficiency has been studied using τ 's from associated bbA^0 production events from the '97sample' and jets (quark and gluon jets) from the 'jets97', applying to them different cut sets, based on the variables R_{em} , ΔE_T^{12} and $N_{tr}(p_T > 2 \text{ GeV})$, to cover τ -identification efficiency values from $\sim 10\%$ to $\sim 90\%$.

Due to the dependence on p_T of the τ -identification criteria, described previously in section 5, jet-rejection vs τ -identification is given for different p_T -ranges.

Fig. 16 and Fig. 17 show how the three variables R_{em} , ΔE_T^{12} and N_{tr} change, changing the cluster p_T -range. The events in each p_T -range were here normalised to 1000 events each: this explains the funny p_T distribution. It is possible to notice that as the p_T gets higher the R_{em} distribution gets narrower both for τ 's and for jets, namely the τ -identification efficiency increases while the jet-rejection decreases. This behaviour can be observed in Fig.18 and Fig.19 in which the τ -identification efficiency and the jet-rejection are represented widening the R_{em} cut.

The jet-rejection vs τ -identification curves are shown in Fig.20, for different cut sets that have been obtained widening gradually the R_{em} , ΔE_T^{12} and N_{tr} cuts.

Since a τ -identification efficiency value can be obtained from different cut combinations, each time the cut combination corresponding to a maximum rejection against jets has been chosen. These criteria imply that not exactly the same cut combinations have been applied in the different p_T ranges to obtain the curves. A straight line fit has been superimposed on each curve.

As expected, the curves shift to higher τ -identification efficiency values as the p_T -range increases. A reasonable approximation of the jet-rejection as function of the τ -efficiency and of p_T is given by:

$$rej = 10^{(0.027+0.00024*p_T)*eff_\tau+(2.28+0.027*p_T)}$$

Taking into account that now cuts have been carefully optimised to have the maximum

jet-rejection, the agreement with the curves given in [2] is not bad.

To complete this study, also the dependence of τ -identification efficiency on η position has been considered. Three η ranges have been considered:

$$0 < |\eta| < 0.7, 0.7 \leq |\eta| \leq 1.5, 1.5 < |\eta| < 2.5.$$

It is possible to observe that the jet-rejection does not depend on η position as we can see in Fig.21 in which jet-rejection values corresponding to different η -regions are plotted for the same τ -identification cuts.

The τ -identification efficiency on the contrary is clearly affected by the η position; in Fig.22 it is possible to notice that the average τ -identification efficiency values in the full η region ($0 < |\eta| < 2.5$) coincide with the values of the $0.7 \leq |\eta| \leq 1.5$ region, but the τ -identification efficiency is higher for central η values and lower for high η values.

A parametrization of this behavior is the following:

$$(eff_{\tau}(0 - 0.7)(in\%) = eff_{\tau}(0.7 - 1.5) * (1.35 - 0.0035 * eff_{\tau}(0.7 - 1.5))$$

$$(eff_{\tau}(1.5 - 2.5)(in\%) = eff_{\tau}(0.7 - 1.5) * (0.70 + 0.0030 * eff_{\tau}(0.7 - 1.5)).$$

This means that the curves of Fig.18 shift towards higher τ -identification efficiencies in the η -region (0-0.7) and towards lower τ -identification efficiencies in the η -region (1.5-2.5), in particular this shift is more evident for narrower τ -identification cuts while the three curves converge as the cuts get wider.

Parametrisations of the jet-rejection vs the τ -identification, considering the dependence on p_T and η , can be useful when the full detector simulation has not been performed. A routine using these parametrisations and giving, for a chosen τ -identification efficiency at a chosen p_T and η , the corresponding jet-rejection has been included in ATLFAST.

8 Effects of underlying event

To understand the effect of the underlying event, we have used the sample of full simulated isolated τ 's. Fig. 23 shows the comparison of the distributions of the quantities used for the τ -identification for isolated τ 's and for τ 's in $bbA^0 \rightarrow \tau\tau$ events, choosing for the latter p_T and η range of τ -jets similar to that one of isolated τ 's.

The distribution of R_{em} in particular is larger for τ 's in complete events: the difference is high also due to the choice of a quite large cone ($R=0.7$) for the jet reconstruction. Such choice influences in particular the quantities calculated in η -strips, where many low energy particles can arrive; see Fig. 24 for the comparison of η -strips quantities for isolated τ 's and for τ 's in events with associated bbA production.

With the criteria used for the A^0 analysis reported in section 5, the τ -identification efficiency for isolated τ 's is about $36\% \pm 2\%$, that is a much higher value with respect to the efficiencies reported in Tab. 2. More precisely, the τ -identification efficiency for τ 's in A^0 events, chosen in the p_T and η range of the isolated τ 's, is $23\% \pm 2\%$ to be compared with the figure quoted above.

9 Effects of cracks

To understand the effect of cracks on τ -identification efficiencies on isolated τ 's and jets, we report briefly as an example the results of a study done in '95 (full simulation done with july 95 DICE version). In particular the region of the crack between the

TILE and the TIXE calorimeter, which corresponded to the region $0.7 < \eta < 1.2$, was studied.

The sample used consists in a set of isolated τ 's and a set of jets generated at a fixed $p_T=100$ GeV from $\eta=0.3$ to $\eta=1.2$ (about 500 events for each η point) to cover the region of interest.

In Fig.25 it is possible to see the τ -identification efficiencies vs η for the two sets of events, using the standard A^0 analysis cuts of section 5. The τ -identification efficiency decreases by 20% for τ 's in the crack region while the jets are not particularly affected by the crack, as expected.

10 τ -veto

The τ -veto can be useful for rejection of standard background (for example $W \rightarrow \tau\nu_\tau$) in the study of SUSY channels. In [2] it was quoted that $\epsilon_{jet} \sim 84\%$ could be achieved with $\epsilon_\tau \sim 14\%$ requesting $N_{tr>(> 2GeV) > 1$ and $R_{em} > 0.12$: the result was integrated on all the p_T of τ 's and jets there used.

A more careful study has now been done in three different p_T ranges. Fig. 26 shows a comparison for $N_{tr>(> 1GeV)$, R_{em} and ΔE_T^{12} for τ 's and jets in the same p_T range. It can immediately be observed that the difference in the three distributions for τ 's and jets decreases from the highest to the lowest p_T range, so the τ -veto performance is expected to be different for different p_T ranges.

The results achieved for the τ -veto are reported in Fig. 27. It can be seen that $\epsilon_{jet} \sim 90\%$ can be achieved with $\epsilon_\tau \sim 5\%$ for $p_T > 60$ GeV, requesting $N_{tr>(> 1GeV) > 3$ and $R_{em} > 0.08$. For lower p_T values, a similar $\epsilon_\tau \sim 5\%$ is obtained with a corresponding lower ϵ_{jet} , decreasing with decreasing p_T ; $\epsilon_{jet} \sim 90\%$ is obtained, but with a not negligible ϵ_τ increasing with decreasing p_T , requesting $N_{tr>(> 1GeV) > 1$ and $R_{em} > 0.12$.

A routine with a parametrisation of the τ -veto from Fig. 27 has also been included in ATLFAST.

11 High luminosity results

It has been verified if the τ identification efficiency for $A^0 \rightarrow \tau\tau$ study can be maintained at its low-luminosity value with a comparable jet-rejection also at high luminosity.

In [3] that was confirmed using an approximate method to evaluate the contribution of pile-up.

Here pile-up events (obtained summing up full simulated minimum bias events weighted through the electronic shaping functions) are added to physical bbA events in calorimeters: energies from the pileup and from the physical event are added at level of each calorimeter cell. An energy cutoff is applied on the energy in each calorimeter tower: towers are built assuming the wider granularity in a given calorimeter and summing longitudinally the cells in that calorimeter. The cutoff applied corresponds to $\sim 2.5\sigma$ of the pileup energy in that tower (that cut has been applied to maintain as much as possible the number of reconstructed jets, the jet energy, the total transverse

energy in calorimeters and the p_T^{miss} resolution similar to the values obtained when the pileup is not added).

Note that R_{em} and ΔE_T^{12} are built using the cell energy content at low luminosity, while here they are built using the calorimeter tower energy content: this procedure gives a less accurate estimate of the two variables, in particular the R_{em} , but allows to apply a less complicate energy cutoff. Note also that we are here assuming that the number of tracks with $p_T > 2$ GeV is not affected by the pile-up addition.

Fig. 28 gives R_{em} , ΔE_T^{12} and N_{tr} distributions for bbA events with $m_A = 450$ GeV at high luminosity compared with the corresponding distributions at low luminosity. It is also given the distribution of τ -jet p_T . Fig. 29 is the same as the previous figure for jets in $t\bar{t}$ events at high and low luminosity. The figures show that the addition of pile-up and the application of calorimeter tower energy cutoff have the effect of enlarging the R_{em} , while the ΔE_T^{12} distribution is narrower.

Table 6 shows that at high luminosity a τ -identification/jet-rejection can be obtained similar to the one obtained at low luminosity, tuning again our analysis cuts.

12 Conclusions

The main results of the study are:

- hadronic decaying τ 's can be very well reconstructed and identified in ATLAS using information both from calorimeters and inner detector
- τ -identification depends on cluster p_T , η and on the underlying event
- by tuning the calorimeter and tracking cuts it is possible to change the τ -identification acceptance and the corresponding jet-rejection
- with a τ -jet identification efficiency of 20% a rejection factor from ~ 170 to ~ 1200 against jets from W+jets and $t\bar{t}$ and ~ 1700 against b-jets can be reached, which allows to have a good sensitivity to the $A^0 \rightarrow \tau\tau$ channel (m_A from 100 to 500 GeV)
- by using the same quantities useful for the τ -identification it is possible to veto the τ -jets ($\sim 5\%$ surviving) with a good acceptance for all other jets ($\sim 90\%$) if the p_T is above ~ 60 GeV
- the τ -identification can be maintained near its low luminosity value with the same jet-rejection also at high luminosity

References

- [1] ATLAS Technical Proposal - 1994
- [2] ATLAS Calorimeter Performance Technical Design Report - 1997
- [3] D. Cavalli, L. Cozzi, L. Perini, S. Resconi - 'Search for $A/H \rightarrow \tau\tau$ Decays' - ATLAS Internal Note PHYS-051 (1994)

- [4] A. Dell'Acqua et al. - '1997 ATLAS Jet Production' - ATLAS Internal Note PHYS-102 (1997)
- [5] ATLAS Inner Detector Technical Design Report - Vol. 1, pag.165 - 1997
- [6] D. Cavalli, S. Resconi - 'Combined single and associated $A/H \rightarrow \tau\tau$ analysis' - ATLAS Internal Note in preparation (1997)

Table 1: *Event sample full simulated for Performance Calorimeter TDR (December 1996) and in 1997*

Events	n^0 events generated	n^0 events detector simulated	sim. time 1 ev. (s) (hp735)	filter cuts
Associated bbA				
$m_A = 100$ GeV	4000	580	~ 1000	$p_T^\mu > 24$ GeV and $ \eta ^\mu < 2.5$ $E_T^{h\tau} > 10$ GeV and $ \eta ^{h\tau} < 2.5$ (where $\tau \rightarrow h_\tau \nu_{\text{tau}}$)
$m_A = 150$ GeV	6000	1200	~ 1150	$E_T^{h\tau} > 30$ GeV and $ \eta ^{h\tau} < 2.5$
$m_A = 300$ GeV	1617	800	~ 1200	"
$m_A = 450$ GeV	810	500	~ 1400	"
Single A				
$m_A = 100$ GeV	4000	566	~ 1100	$E_T^{h\tau} > 10$ GeV and $ \eta ^{h\tau} < 2.5$
$m_A = 100$ GeV	9524	600	~ 1300	$E_T^{h\tau} > 30$ GeV and $ \eta ^{h\tau} < 2.5$
$m_A = 150$ GeV	7400	1500	~ 1400	"
	2500	500 (in $ \eta < 5.$)	~ 2400	"
$m_A = 300$ GeV	1654	774	~ 1900	"
$m_A = 450$ GeV	1000	508	~ 2200	"
$Z \rightarrow \tau\tau$	55879	1500	~ 800	"
$t\bar{t} (\rightarrow W \rightarrow jets)$	3305	800	~ 2200	$p_T^\mu > 24$ GeV and $ \eta ^\mu < 2.5$ $m_T(\mu - p_T^{miss}) < 50$ GeV
W+jets	12500	1100	~ 1100	$p_T^\mu > 24$ GeV and $ \eta ^\mu < 2.5$ $m_T(\mu - p_T^{miss}) < 50$ GeV at least 1 string with $p_T > 30$ GeV
$b\bar{b}$	200000	504	~ 1400	$p_T^\mu > 24$ GeV and $ \eta ^\mu < 2.5$ $\hat{p}_T > 15$ GeV

Table 2: Efficiency (in %) of τ -identification criteria for hadronic τ -decays and for jet backgrounds at low luminosity ('97sample' and 'jets97').

Variable	Cut	bbA \rightarrow $\tau\tau$	A \rightarrow $\tau\tau$	'jets97'	b-jets	$t\bar{t}$	W+jets
$\langle p_T \rangle$ (GeV)		80.	73.	44.	58.	65.	52.
R_{em}	< 0.07	56. \pm 1.	45. \pm 1.	1.1 \pm 0.1	1.9 \pm 0.4	1.3 \pm 0.2	2.9 \pm 0.5
ΔE_T^{12}	< 0.1	40. \pm 1.	32. \pm 1.	0.6 \pm 0.05	0.9 \pm 0.2	0.7 \pm 0.2	1.8 \pm 0.5
$N_{tr}, p_T > 2$	$= 1$	21. \pm 1.	17. \pm 1.	0.09 \pm 0.02	< 0.06	0.08 \pm 0.06	0.6 \pm 0.3
$N_{tr}, p_T > 2$	$= 1$ or 3	32. \pm 1.	25. \pm 1.	0.19 \pm 0.03	0.18 \pm 0.1	0.2 \pm 0.1	1.08 \pm 0.3
$N_{tr}, p_T > 1$	$= 1$	20. \pm 1.	16. \pm 1.	0.08 \pm 0.02	< 0.06	0.08 \pm 0.06	0.6 \pm 0.3
$N_{tr}, p_T > 1$	$= 1$ or 3	32. \pm 1.	25. \pm 1.	0.13 \pm 0.02	0.24 \pm 0.1	0.2 \pm 0.1	1.08 \pm 0.3
$N_{tr}, p_T > 5$	$= 1$	20. \pm 1.	16. \pm 1.	0.14 \pm 0.03	0.12 \pm 0.1	0.04 \pm 0.4	0.9 \pm 0.3
$N_{tr}, p_T > 5$	$= 1$ or 3	28. \pm 1.	23. \pm 1.	0.21 \pm 0.03	0.3 \pm 0.1	0.11 \pm 0.7	1. \pm 0.3

Table 3: Efficiency (in %) of τ -identification criteria for hadronic τ -decays and for jet backgrounds at low luminosity ('TPsample').

Variable	Cut	A \rightarrow $\tau\tau$	b-jets	Other jets
$\langle p_T \rangle$ (GeV)		71.	65.	73.
R_{em}	< 0.07	41	0.8	1.2
ΔE_T^{12}	< 0.1	27	0.4	0.7
$N_{tr}, p_T > 2$	$= 1$	24	0.05	0.25

Table 4: *Expected numbers of events for signal and backgrounds and combined significance after kinematic cuts, but before τ -identification cuts, for an integrated luminosity of $3 * 10^4 pb^{-1}$ and $tg(\beta)=10$. The first number refers to the 'a2' analysis the second one to the 'a1' analysis. (A^0 means $A^0 + H^0$)*

Signal mass (GeV) Mass bin (GeV)	$m(A^0)=150$ 115-165	$m(A^0)=300$ 245-355	$m(A^0)=450$ 375-525
$\sigma(\text{single } A^0)$ for $tg(\beta)=10$ (pb)	1.26	0.05	0.015
Single A^0 signal for $tg(\beta)=10$	8 403	– 48	0.08 0.7
$\sigma(b\bar{b}A^0)$ for $tg(\beta)=10$ (pb)	2.93	0.28	0.04
$b\bar{b}A^0$ signal for $tg(\beta)=10$	327 308	108 57	2 0.7
W+jets	– 138240	– 414720	– 414720
$t\bar{t}(\rightarrow W \rightarrow jets)$	1497 4488	1497 2991	1497 2991
$t\bar{t}(\rightarrow W \rightarrow \tau)$	633 705	1128 633	351 633
$b\bar{b}$	86786 173571	86786 86786	86786 86786
$Z^0 \rightarrow \tau\tau$	303 2436	– –	– –
Combined significance	1.7	0.4	0.007

Table 5: *Expected numbers of events and combined significances for $A^0/H^0 \rightarrow \tau\tau$ channel, after all cuts, for an integrated luminosity of $3 * 10^4 pb^{-1}$ and $tg(\beta)=10$. The first number refers to the 'a2' analysis the second one to the 'a1' analysis.*

Signal mass (GeV) Mass bin (GeV)	$m(A^0)=150$ 115-165	$m(A^0)=300$ 245-355	$m(A^0)=450$ 375-525
Single A^0 signal for $tg(\beta)=10$	0 55	0 9	0 0.15
$b\bar{b}A^0$ signal for $tg(\beta)=10$	88 56	18 6	0.63 0.13
Total background	57 1314	61 2749	56 955
Combined significance $N_{tr} = 1$	12.3	2.3	0.08
Combined significance $N_{tr}=1$ or 3	8.8	2.5	0.07
5σ limit on $tg(\beta)$	6.5 ± 1.3	14.6 ± 2.9	22.6 ± 4.5

Table 6: *Efficiency (in %) of τ -identification criteria for hadronic τ -decays ($m_A=450$ GeV) and for jet backgrounds at high luminosity.*

Variable	Old cuts	bbA \rightarrow $\tau\tau$ $m_A=450$ GeV low	bbA \rightarrow $\tau\tau$ $m_A=450$ GeV high	$t\bar{t}$ low	$t\bar{t}$ high	New cuts	bbA \rightarrow $\tau\tau$ high	$t\bar{t}$ high
R_{em}	< 0.07	72	52	1.27	2.7	< 0.12	78	18
ΔE_T^{12}	< 0.1	53	43	0.72	1.2	< 0.08	51	2.3
N_{tr}	$= 1$	26	21	0.08	0.08	$= 1$	24	0.08

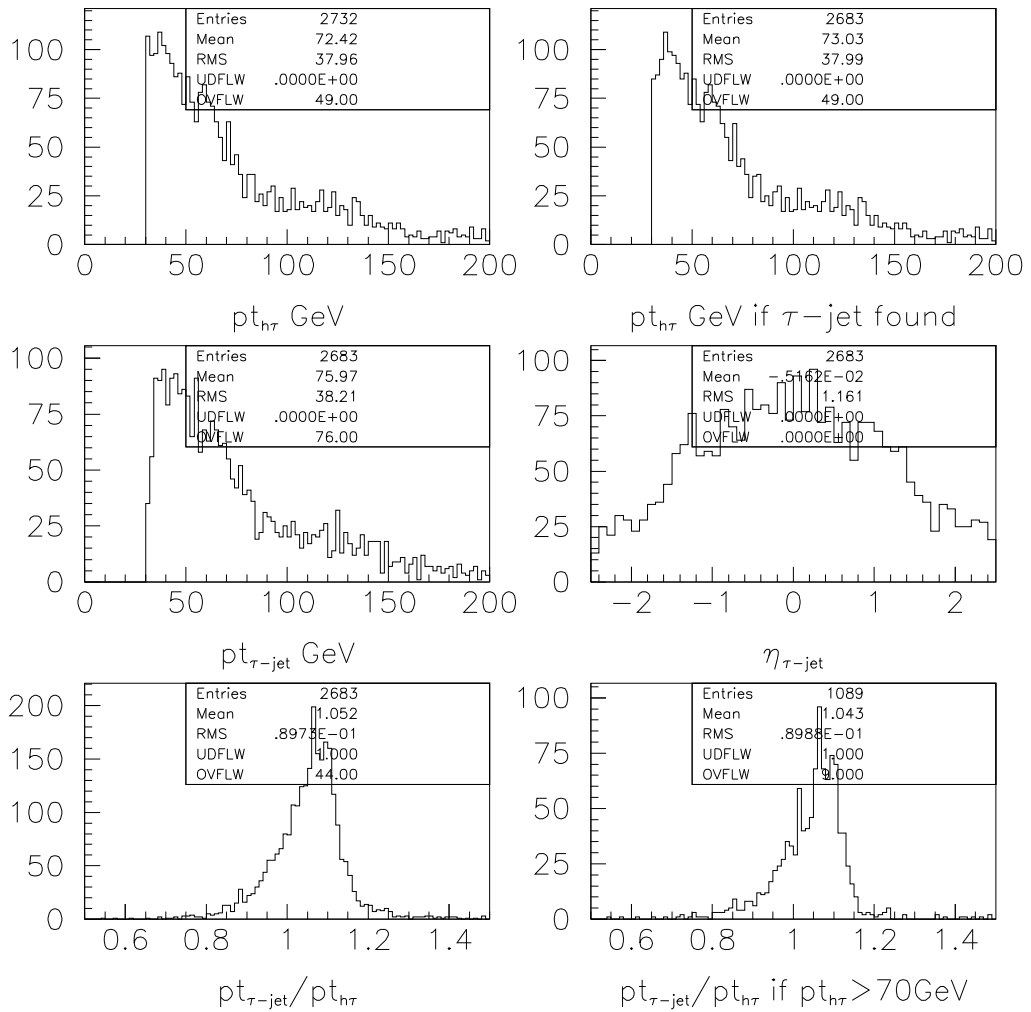


Figure 1: *Distributions of $p_T(h_\tau)$ and $p_T(\tau\text{-jet})$ and their ratio*

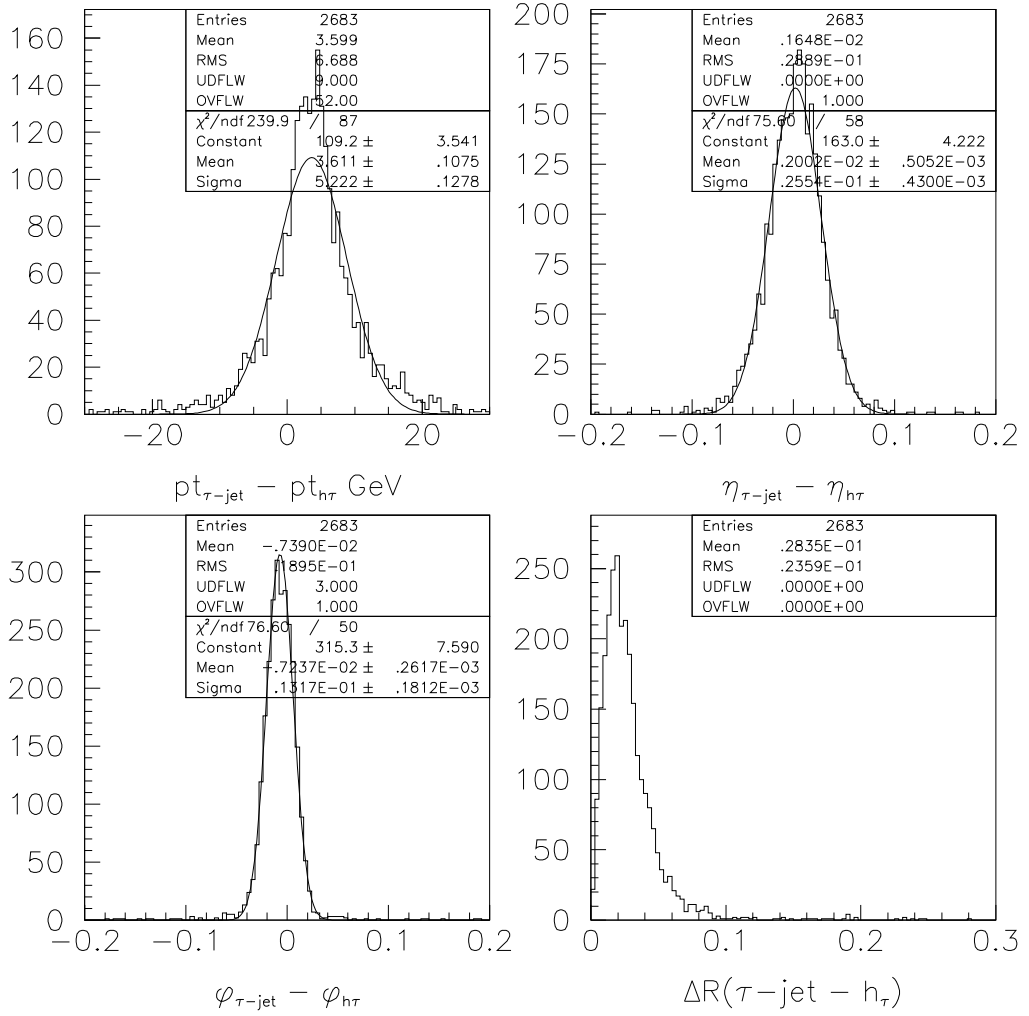


Figure 2: Resolutions of energy and direction measurement of τ -jets

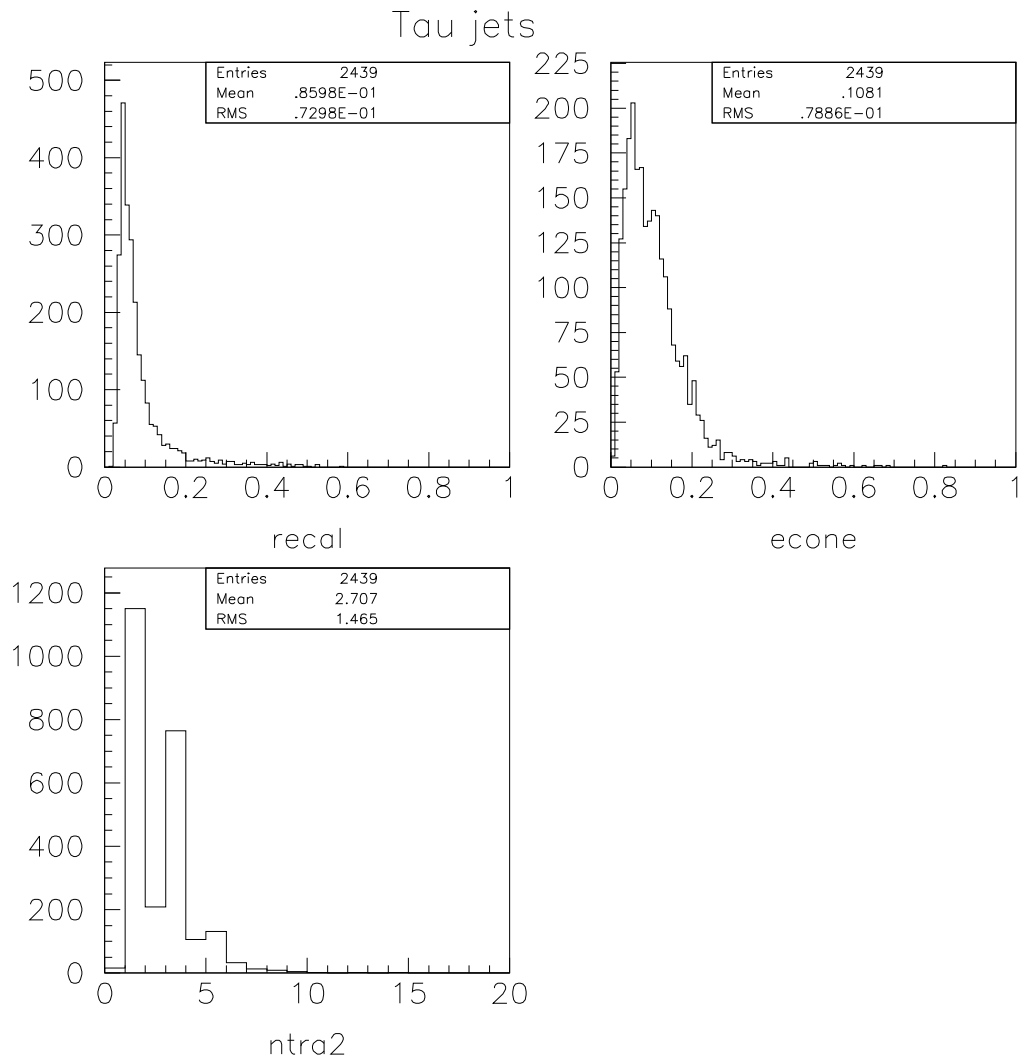


Figure 3: Distributions of the τ -identification variables Rem , ΔE_T^{12} and N_{tr} with $p_T > 2$ GeV for τ -jets from bbA^0 production ('97sample')

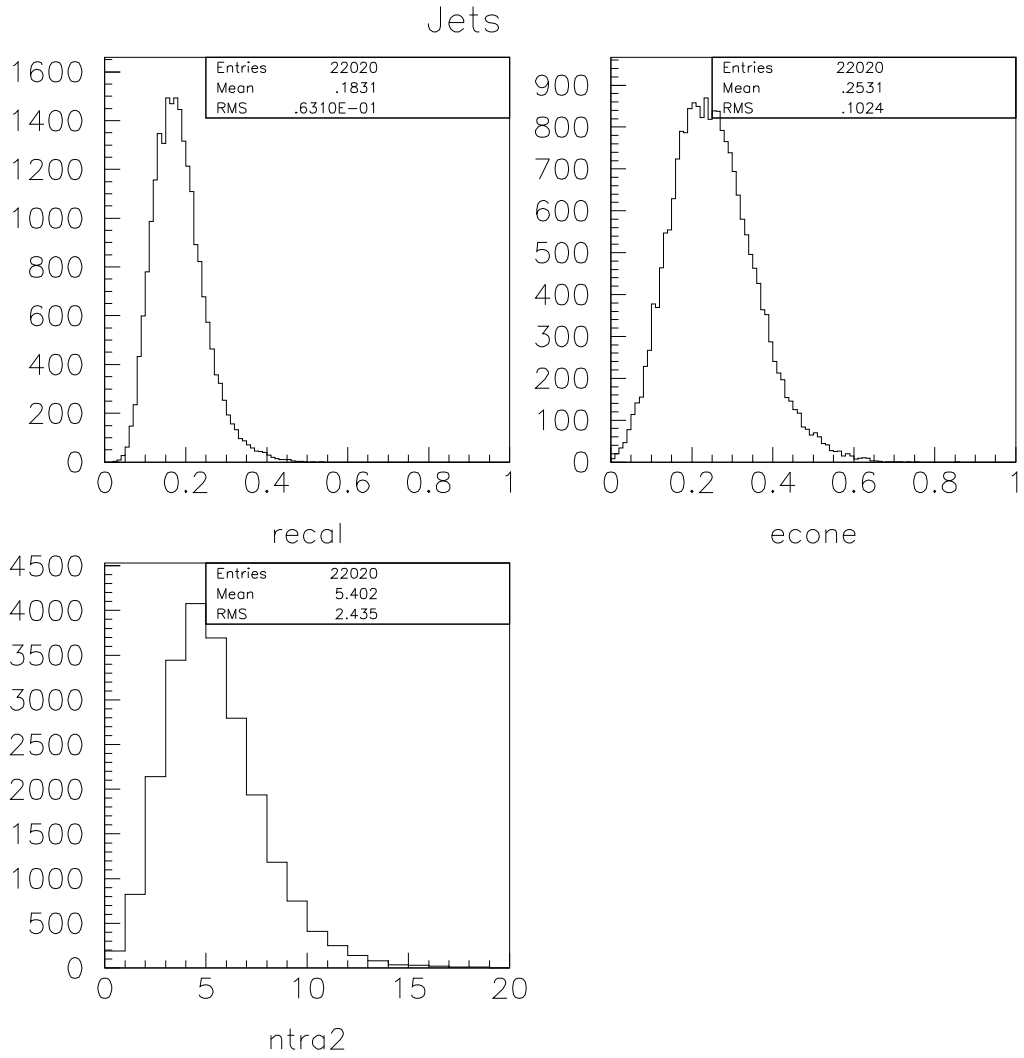


Figure 4: *Distributions of the τ -identification variables Rem , ΔE_T^{12} and N_{tr} with $p_T > 2$ GeV for jets from the large 97 jet-sample ('jets97')*

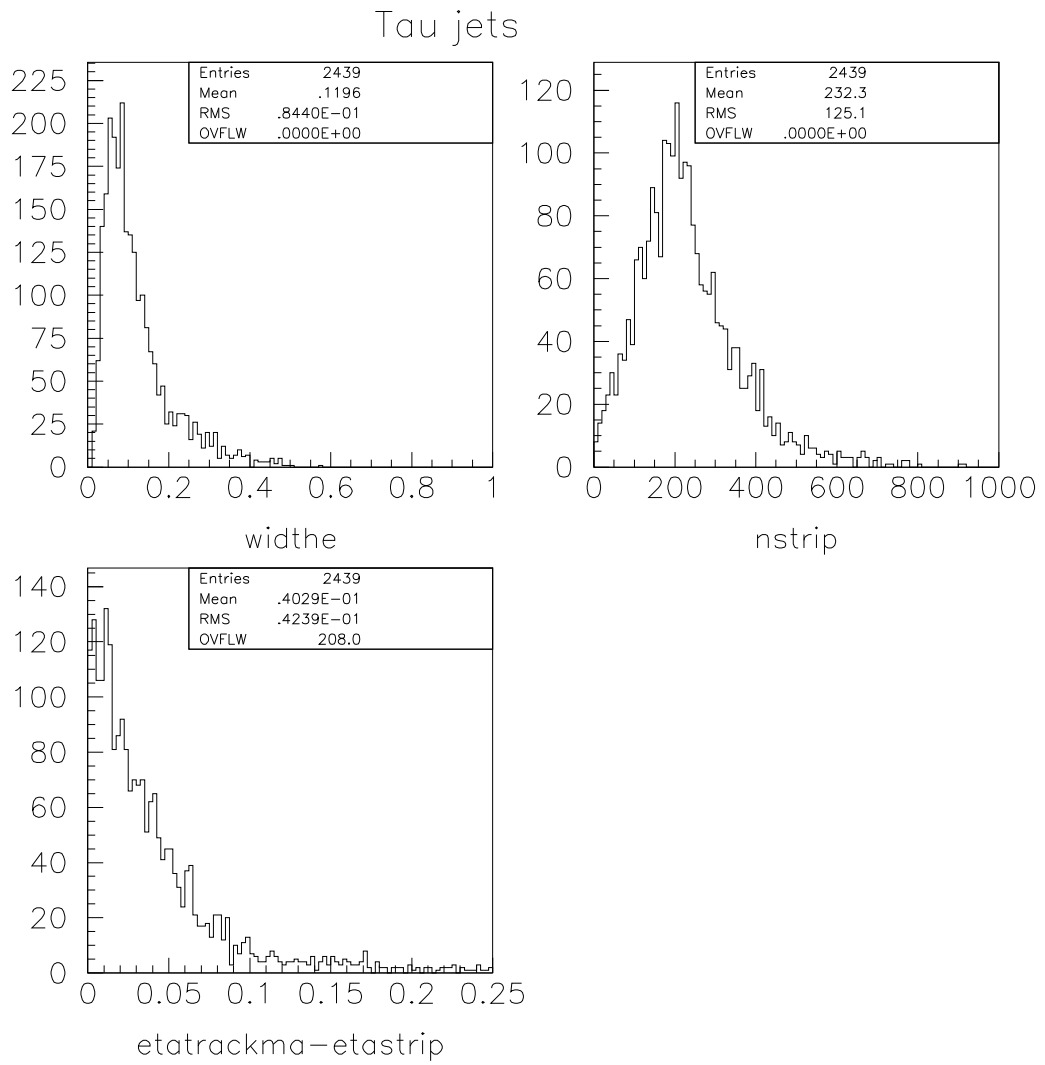


Figure 5: *Distributions of the variables η -width, N_{strip} and $distri$ for τ -jets from bbA^0 production ('97sample')*

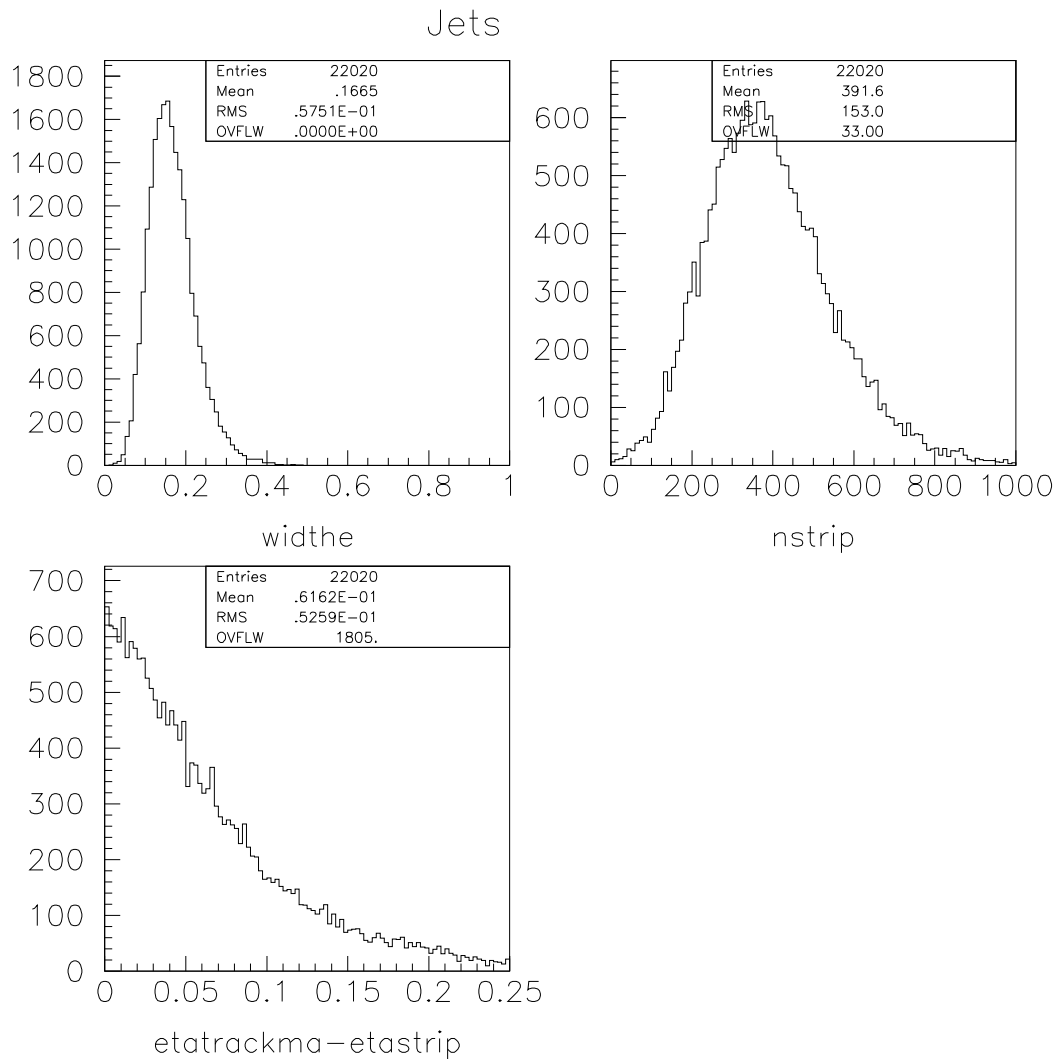


Figure 6: *Distributions of the variables η -width, N_{strip} and $distri$ for jets ('jets97')*

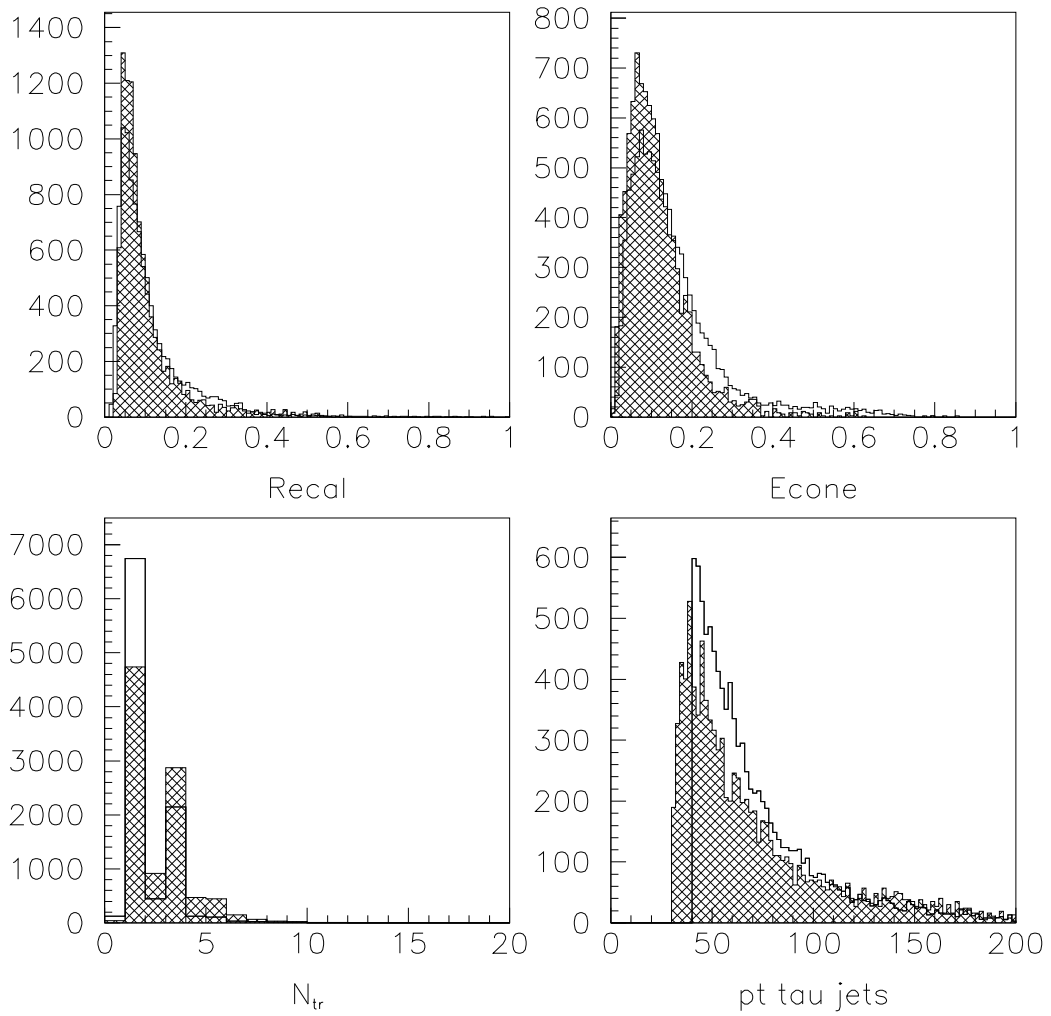


Figure 7: Comparison between τ 's in 'TPsample' and '97sample' (dashed histograms); distributions are normalised to the same number of events

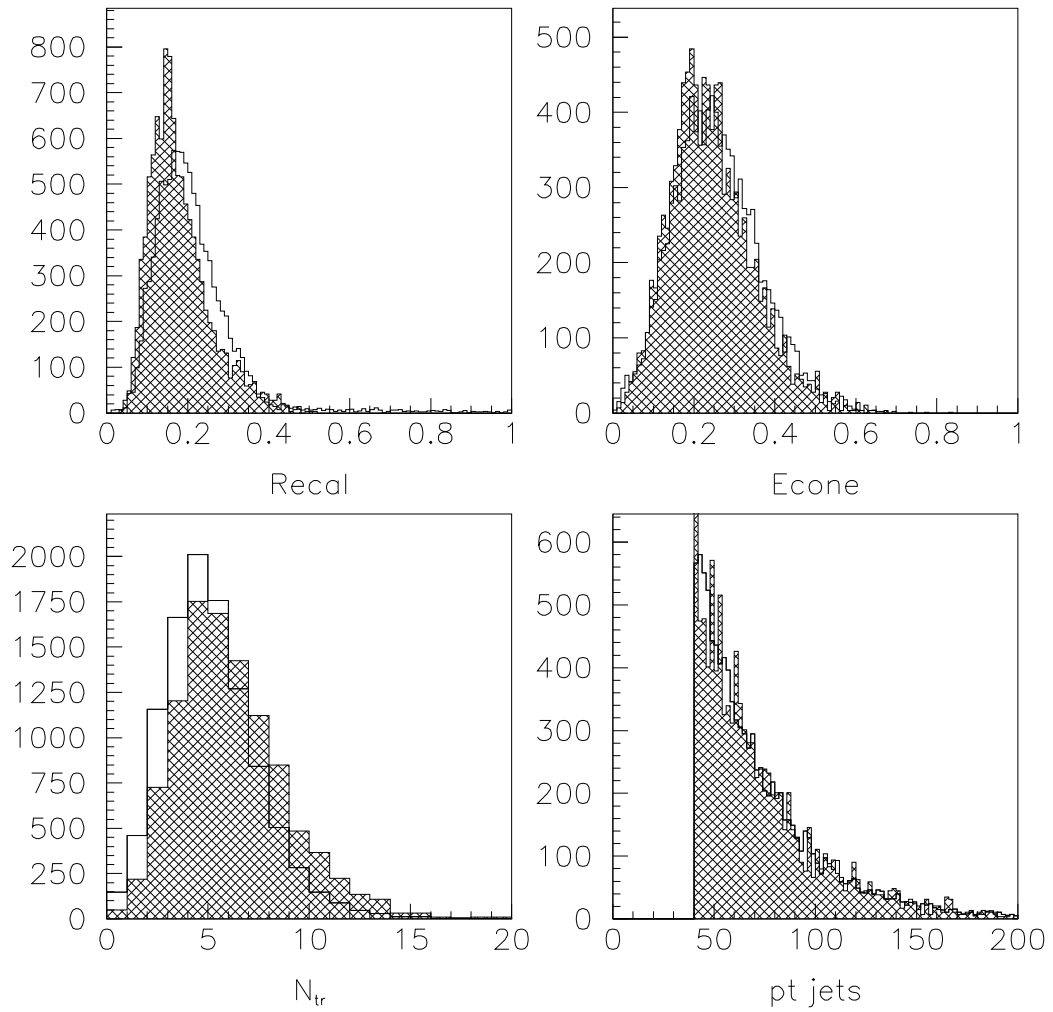


Figure 8: Comparison between jets in 'TPsample' and '97sample' (dashed histograms); distributions are normalised to the same number of events

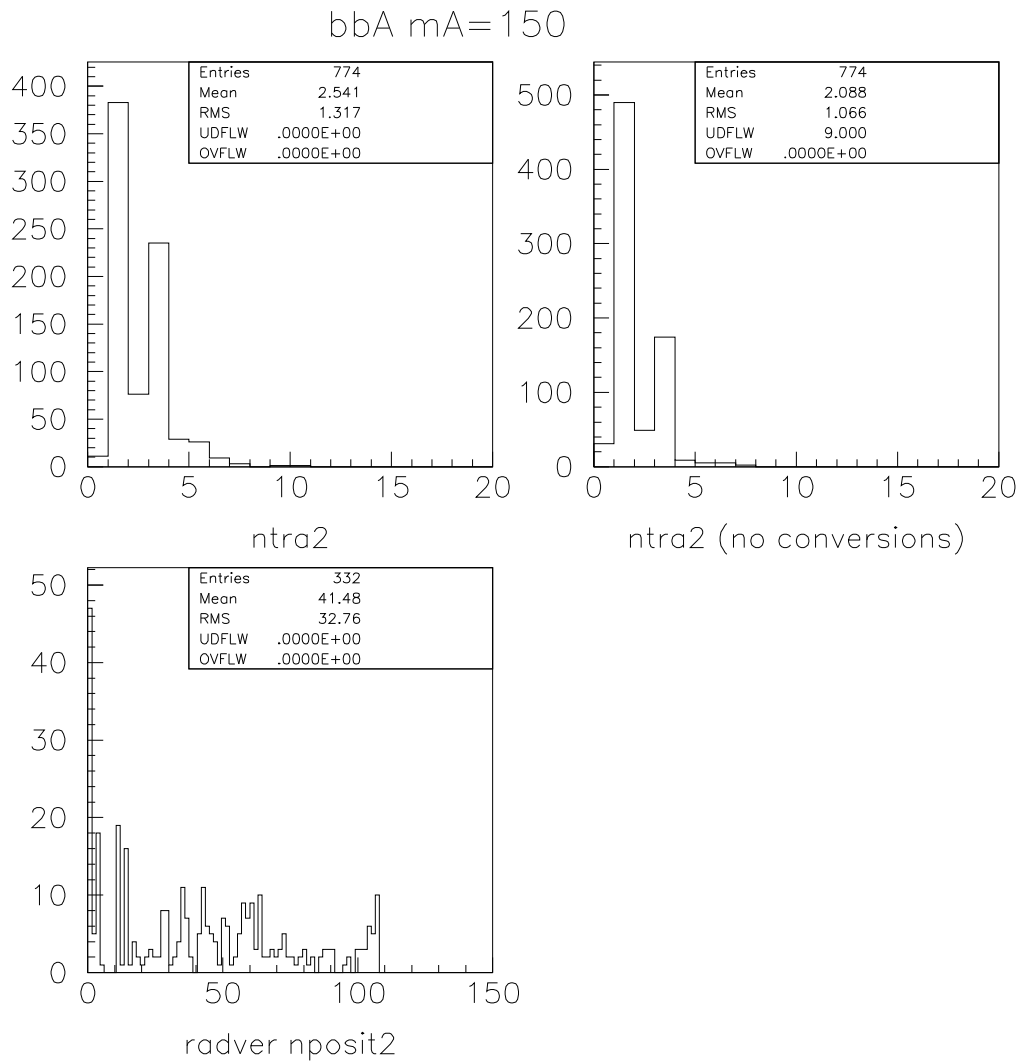


Figure 9: Comparison between associated charged tracks to τ -jet with and without the tracks from γ conversion; distribution of the vertex of associated positrons with $p_T > 2$ GeV

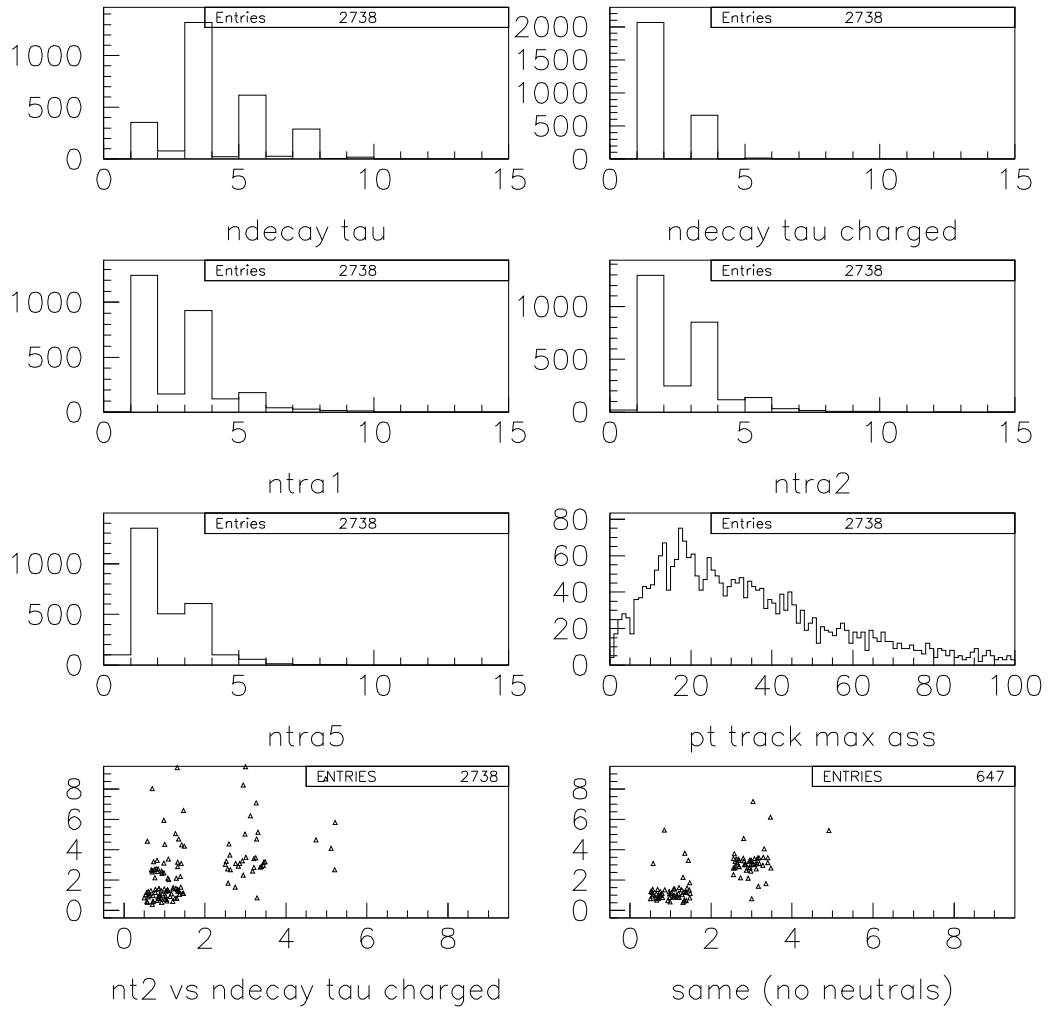


Figure 10: Comparison between the number of particles from τ hadronic decay and the number of associated charged tracks to τ -jet (with various p_T cuts: 1, 2, 5 GeV)

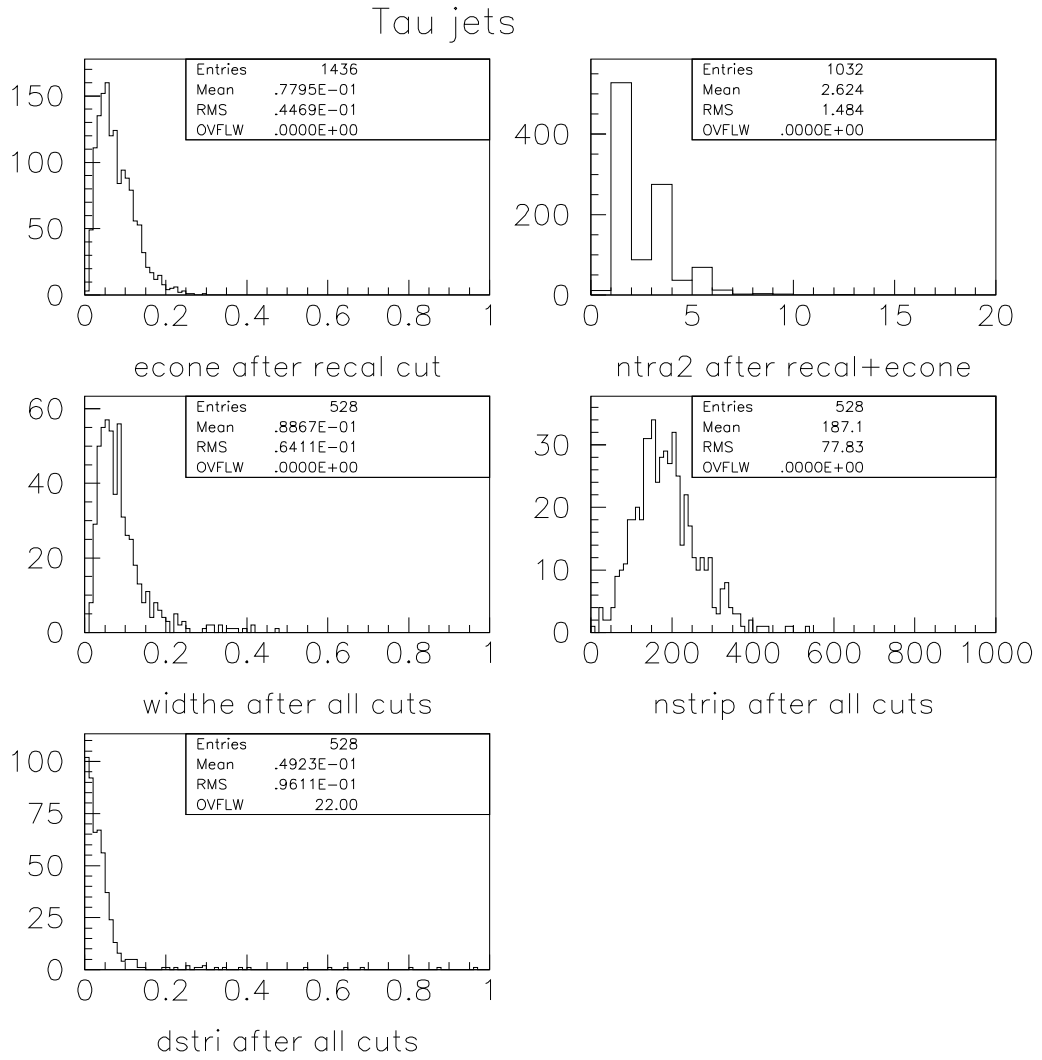


Figure 11: *Distributions of the variables ΔE_T^{12} , N_{tr} with $p_T > 2$ GeV, η -width, N_{strip} and $dstri$ for τ -jets from bbA^0 production after the τ -identification cuts applied sequentially*

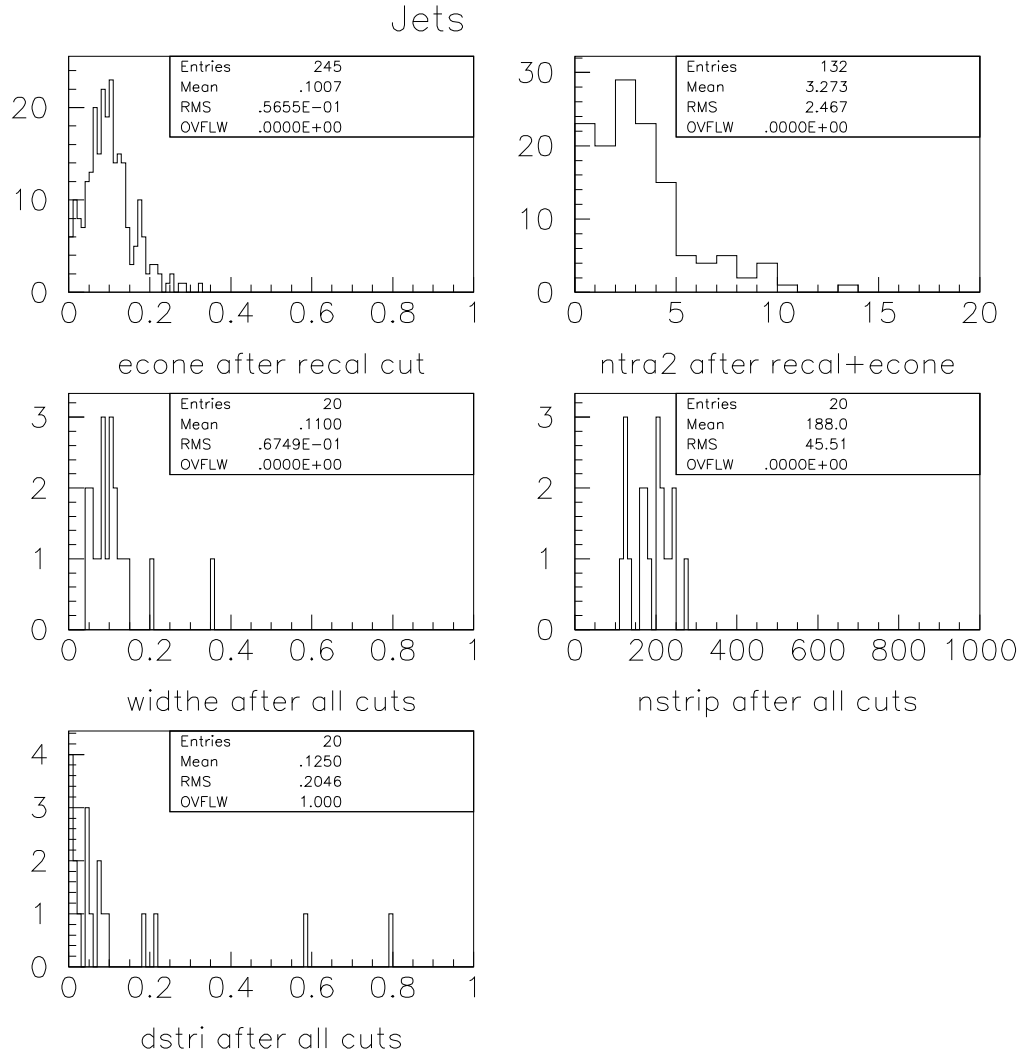


Figure 12: *Distributions of the variables ΔE_T^{12} , N_{tr} with $p_T > 2$ GeV, η -width, N_{strip} and $dstri$ for jets after τ -identification cuts applied sequentially*

compare REC tracks (full) with KINE tracks (dashed)

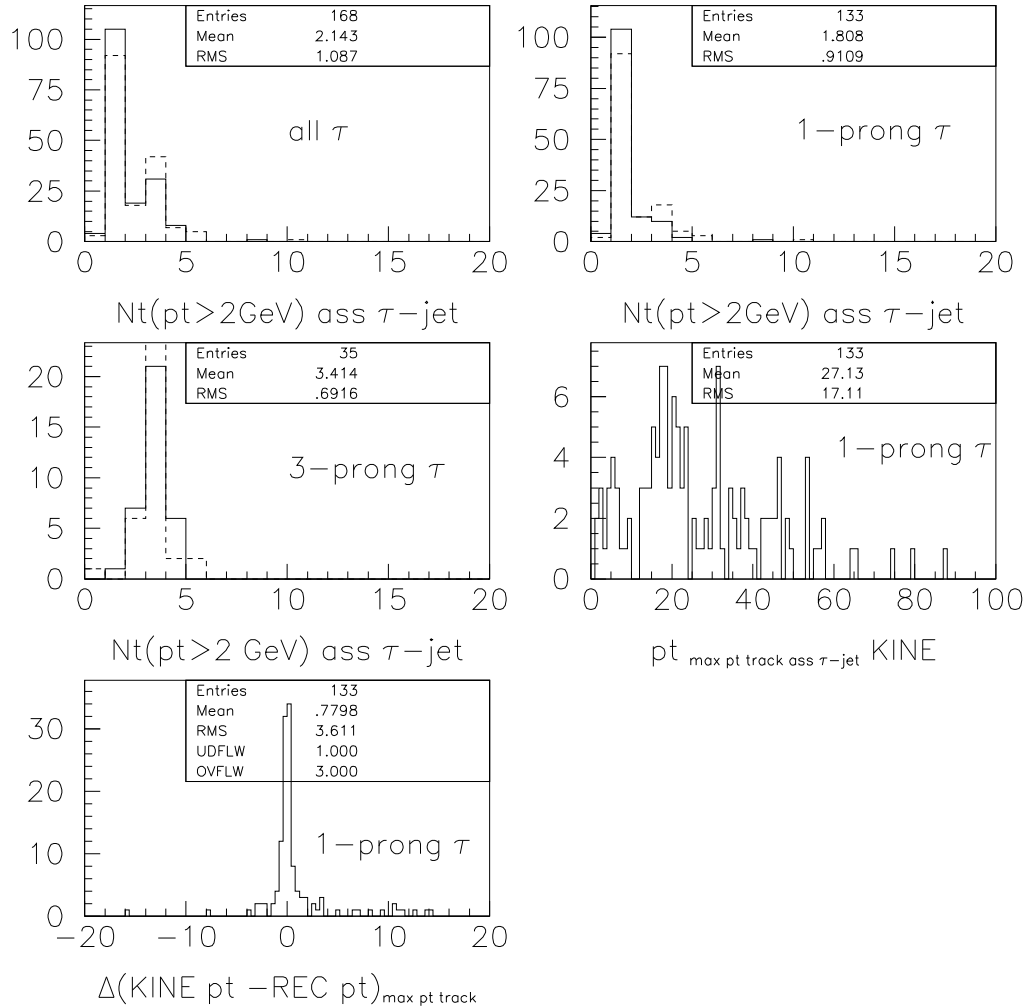


Figure 13: Comparison of number of reconstructed tracks (full line) and tracks from KINE bank (dashed line) for all τ 's, 1-charged-prong τ 's and 3-charged-prong τ 's; p_T of maximum p_T associated KINE track for 1-charged-prong τ 's and difference between reconstructed and KINE p_T of the maximum p_T associated track

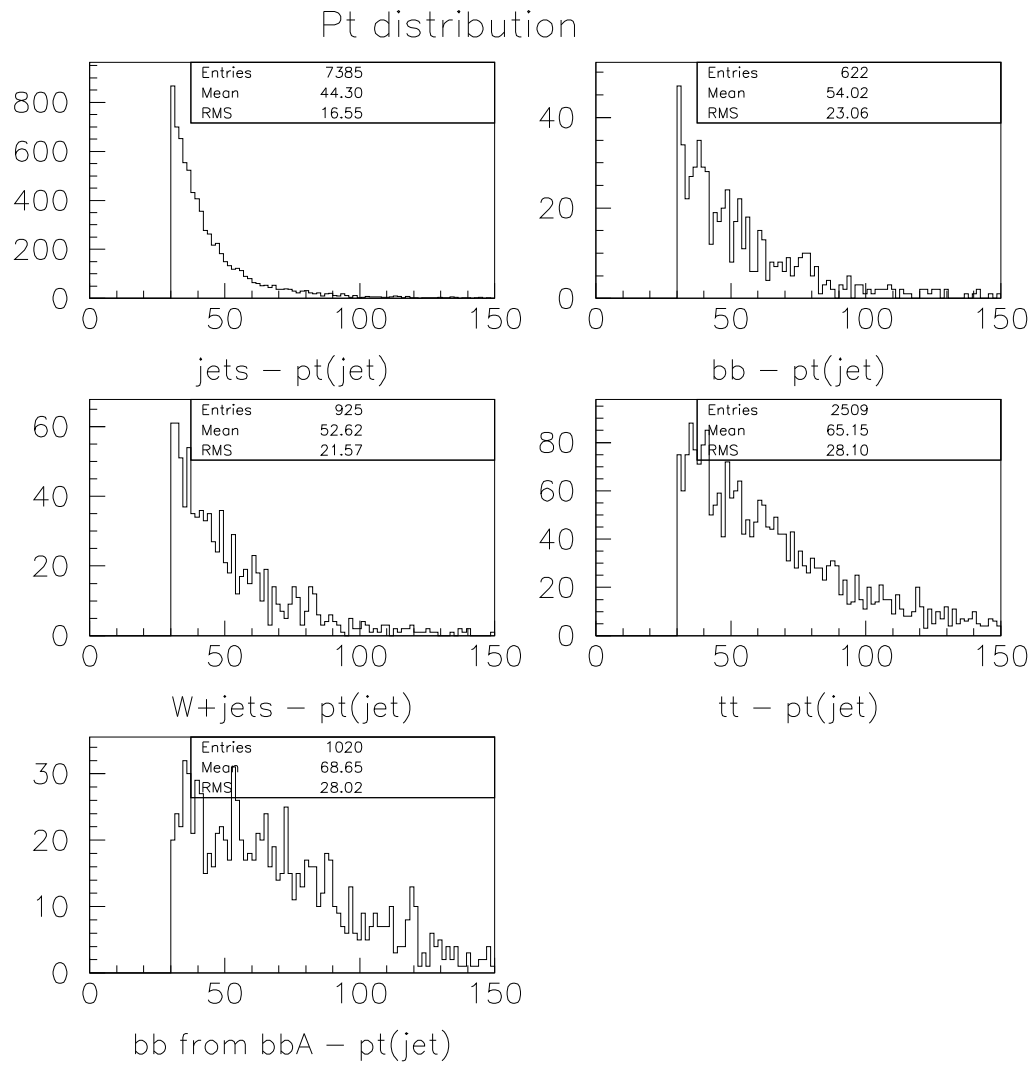


Figure 14: *Pt* distribution of different jet samples used ('jets97' + jets from A^0 backgrounds '97sample')

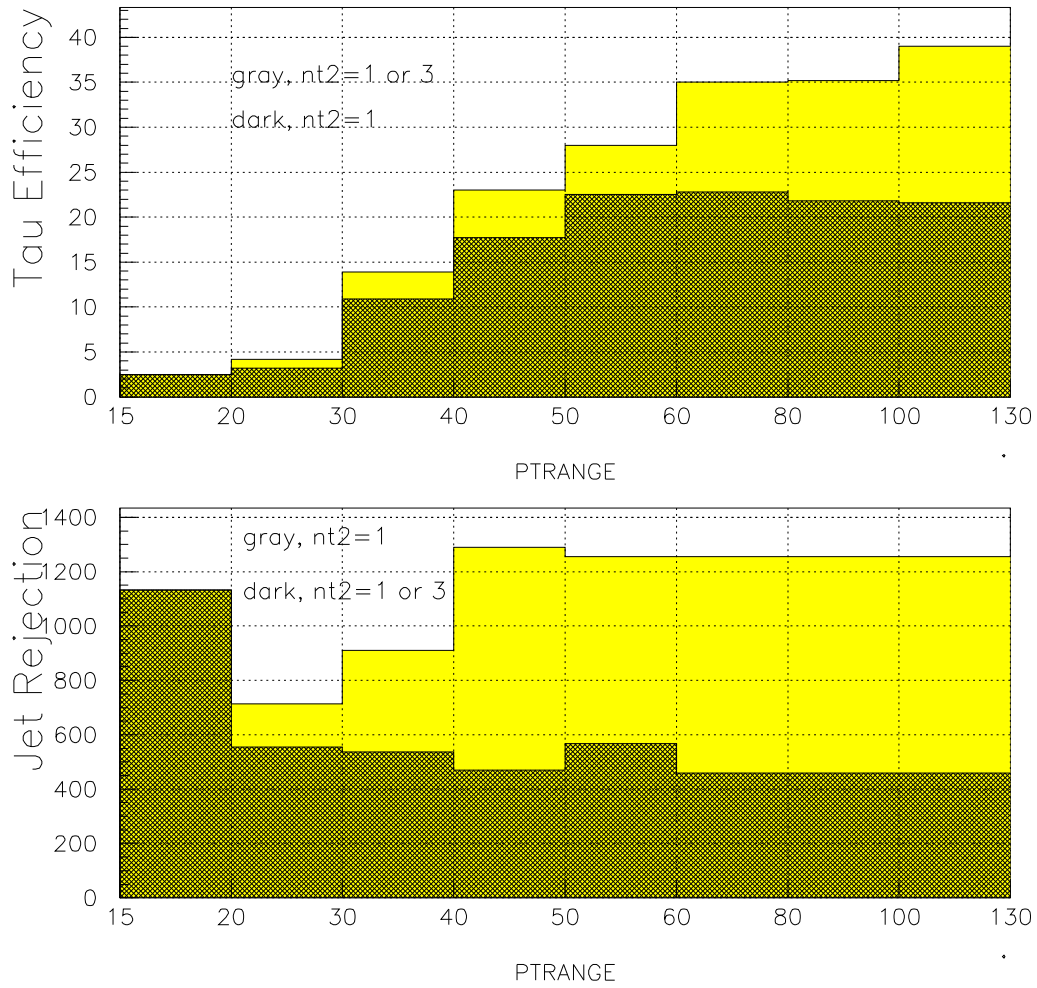


Figure 15: τ efficiency and jet-rejection vs p_T applying same cuts as in $A^0 \rightarrow \tau\tau$ analysis

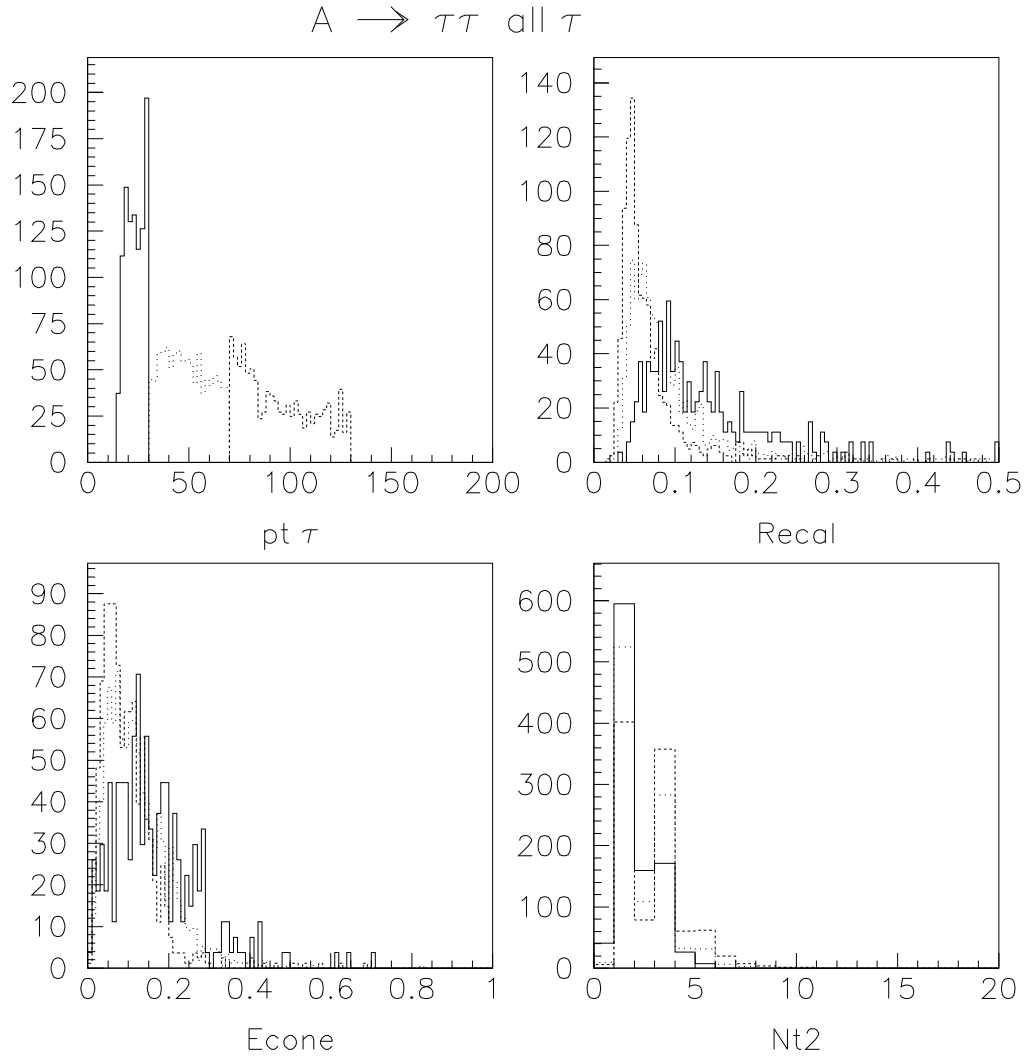


Figure 16: R_{em} , ΔE_T^{12} and N_{tr} in different p_T ranges for τ -jets

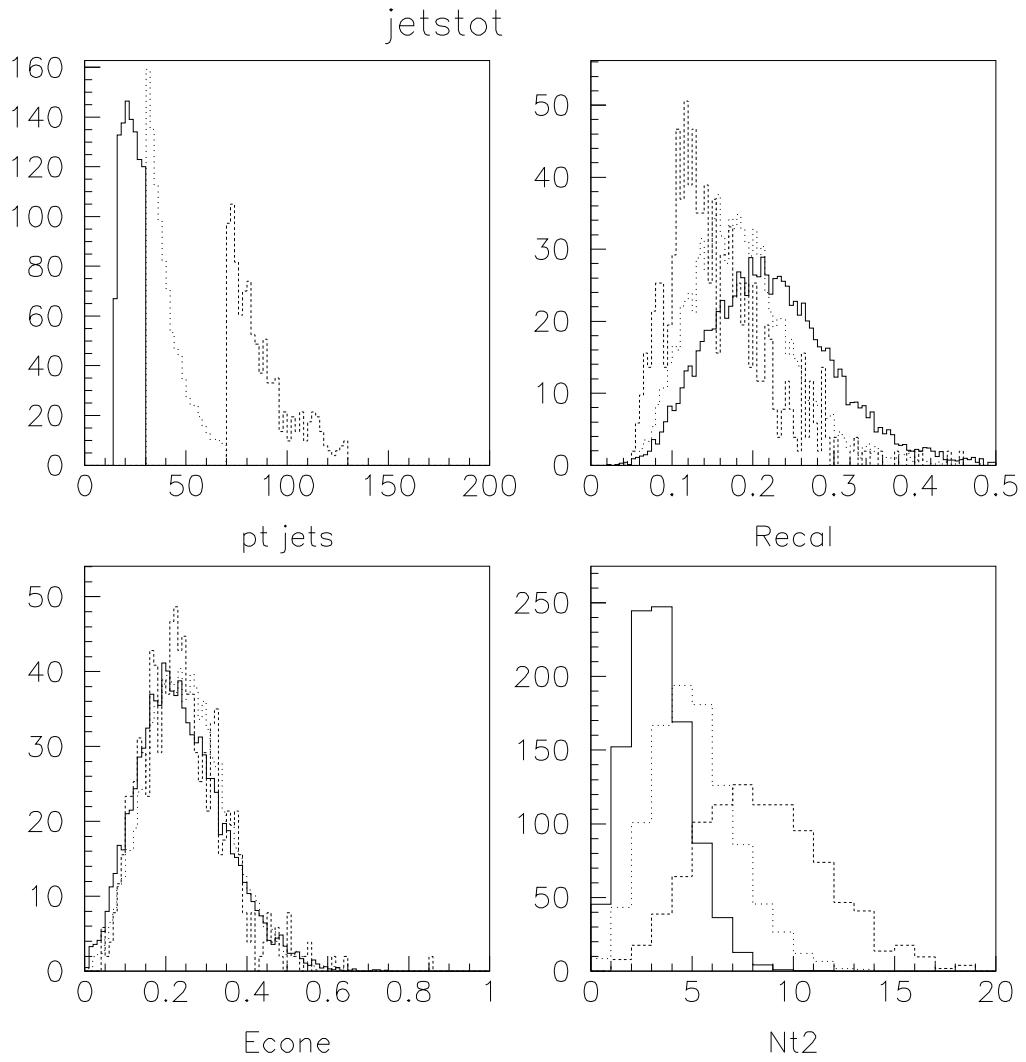


Figure 17: R_{em} , ΔE_T^{12} and N_{tr} in different p_T ranges for jets

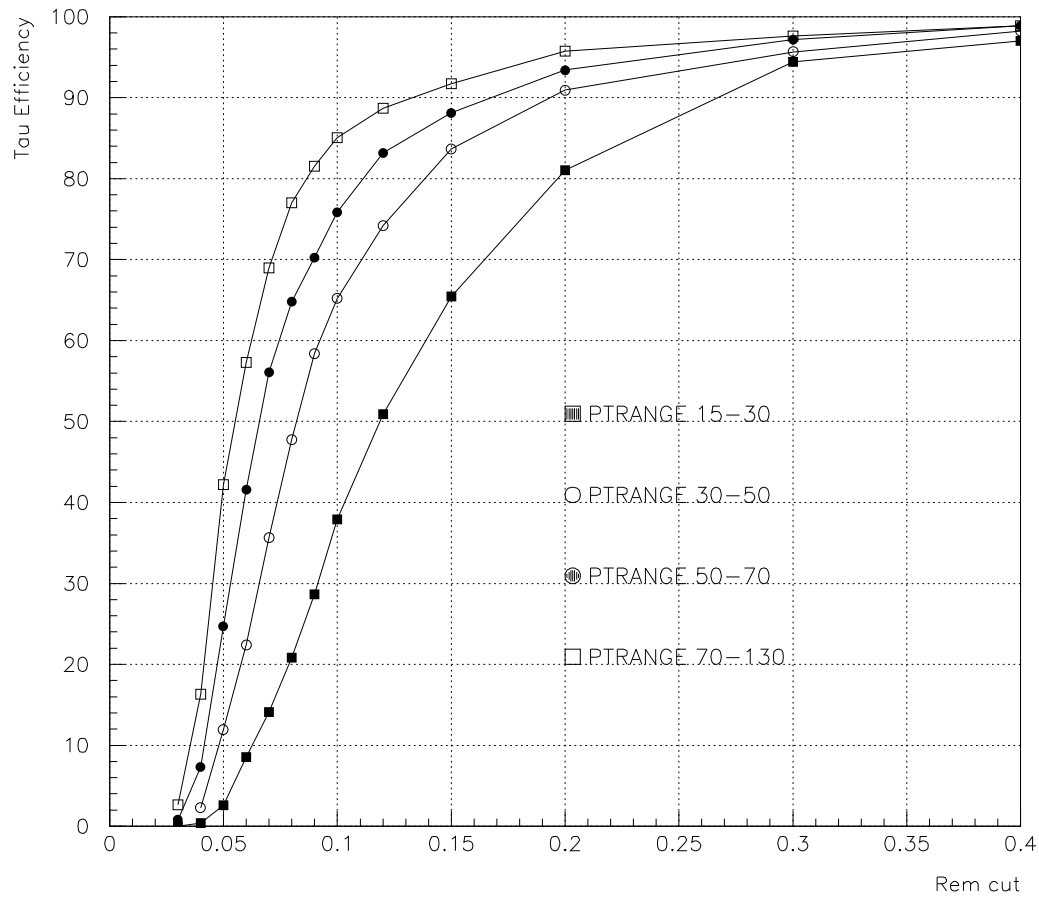


Figure 18: τ -identification efficiency for different p_T -ranges vs R_{em} cut

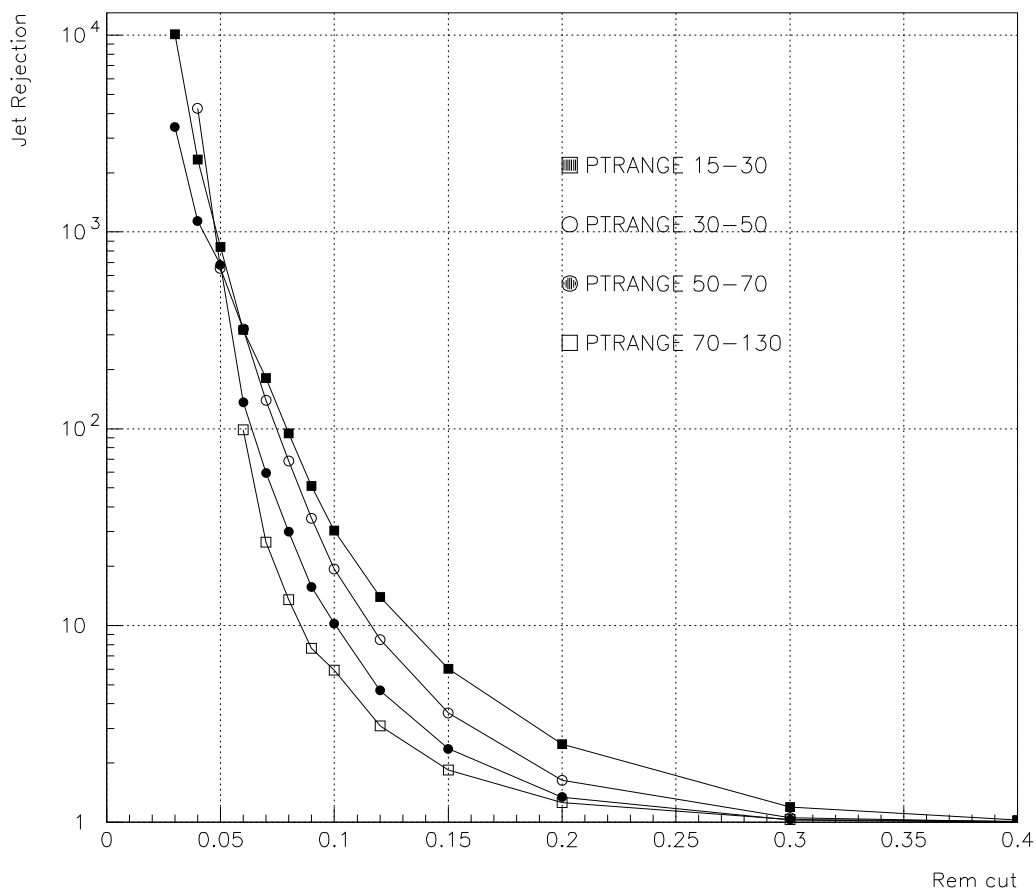


Figure 19: *jet-rejection for different p_T -ranges vs R_{em} cut*

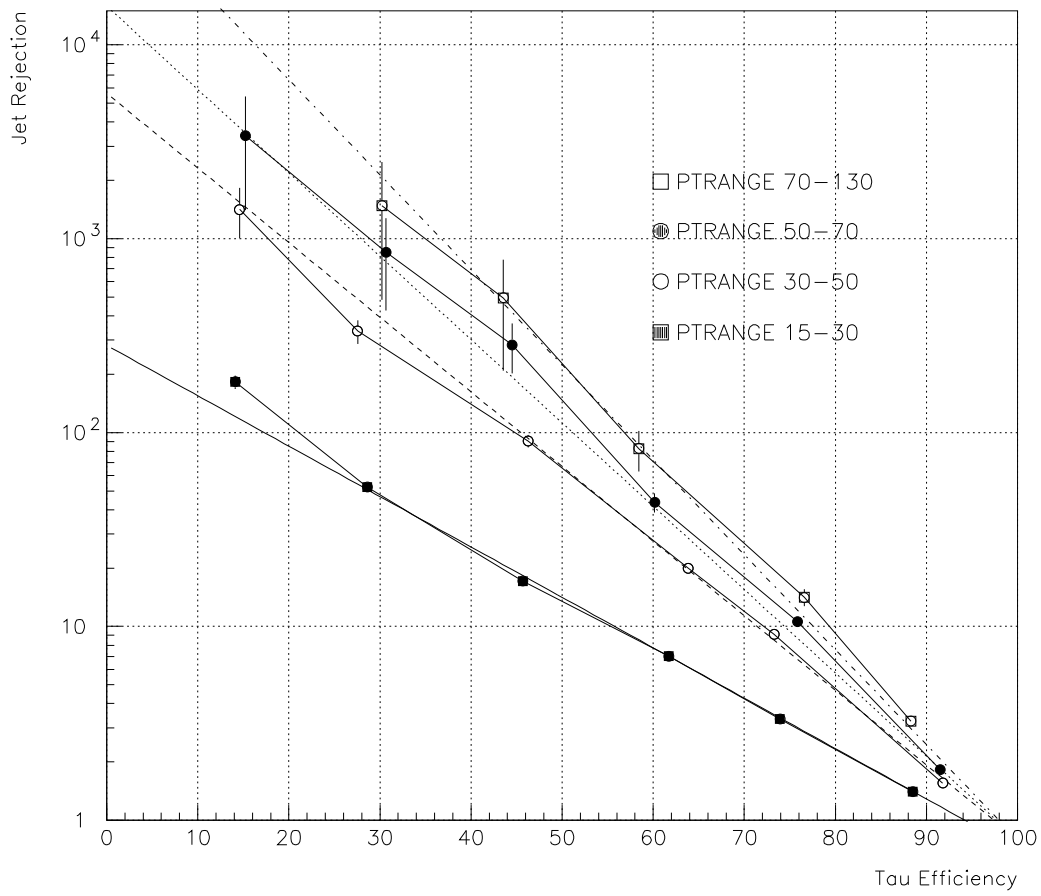


Figure 20: *jet-rejection vs τ efficiency for different p_T -ranges*

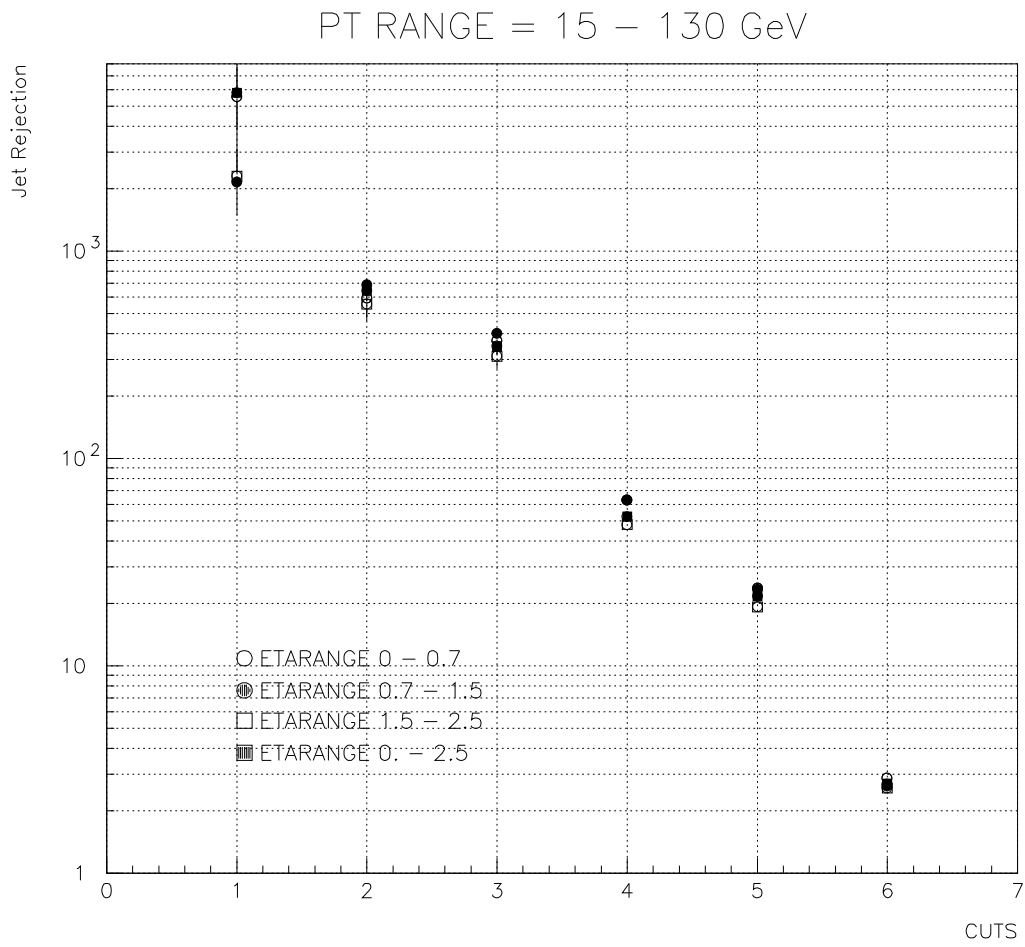


Figure 21: *jet-rejection for different η regions varying the τ -identification cuts*

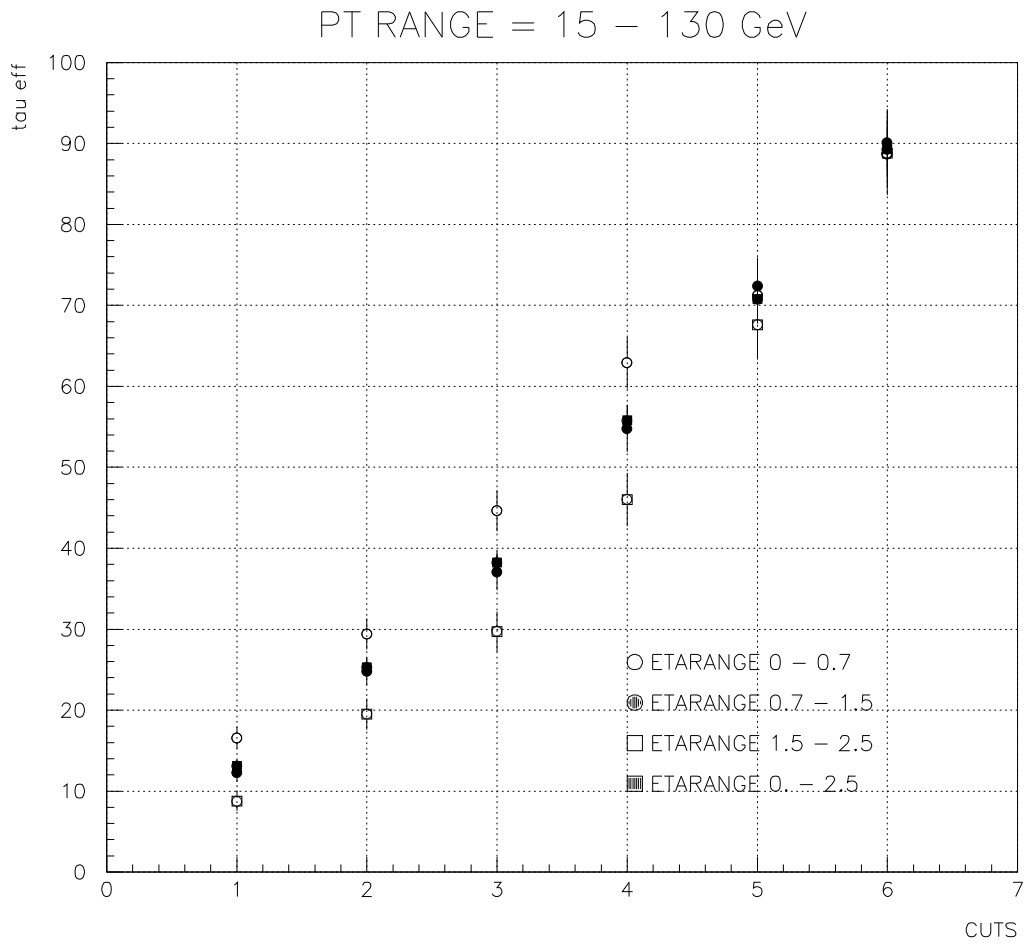


Figure 22: τ -identification efficiencies for different η regions varying the τ -identification cuts

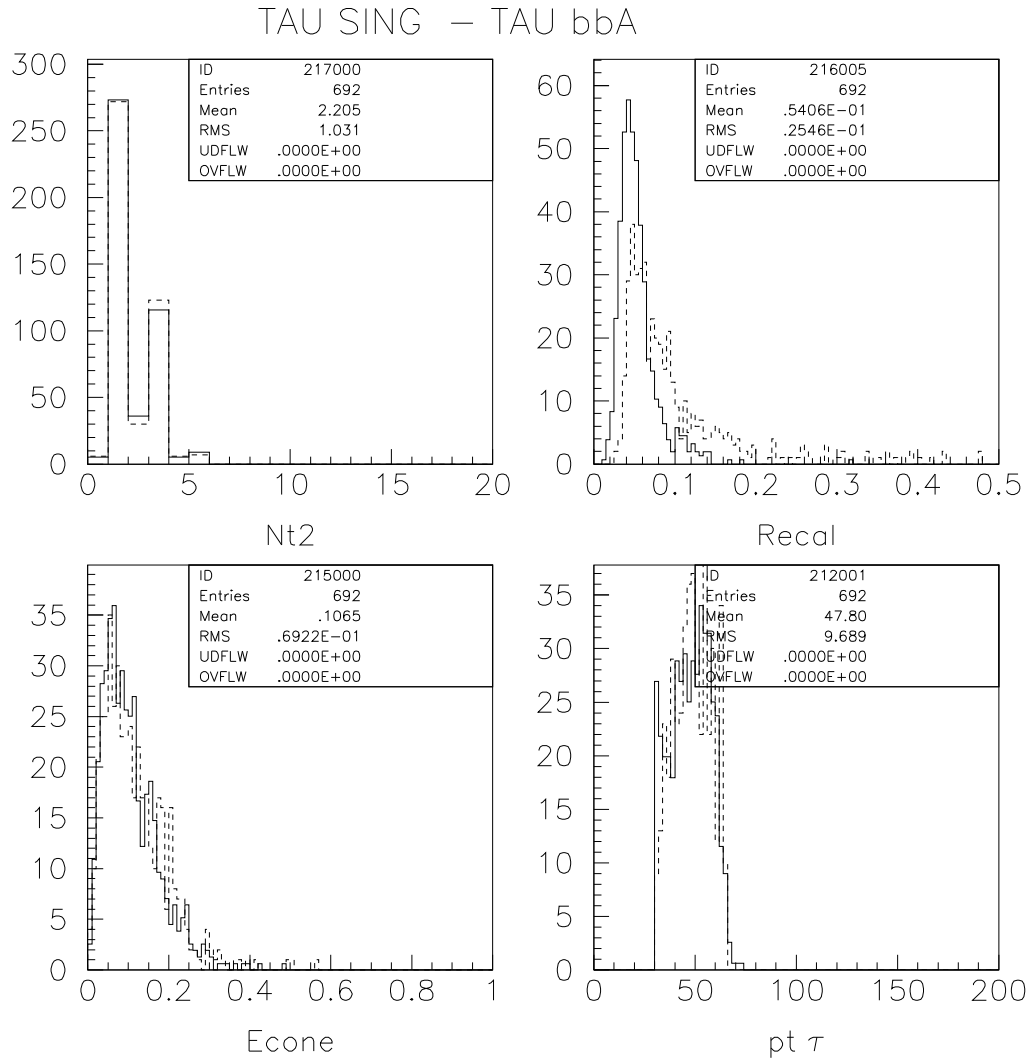


Figure 23: R_{em} , ΔE_T^{12} and N_{tr} for isolated τ 's (full line) and τ 's in bbA events (dashed line)

TAU SING – TAU bbA

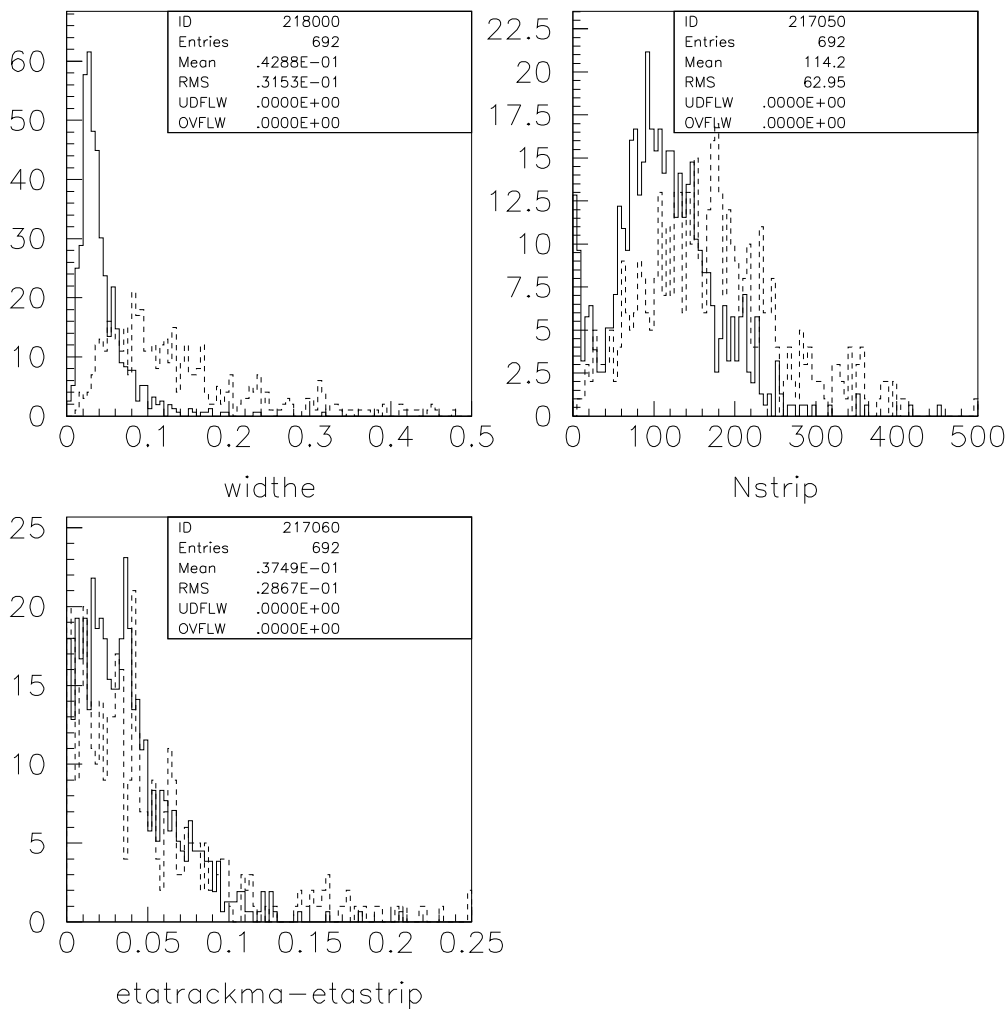


Figure 24: η -strips quantities for isolated τ 's (full line) and τ 's in bbA events (dashed line)

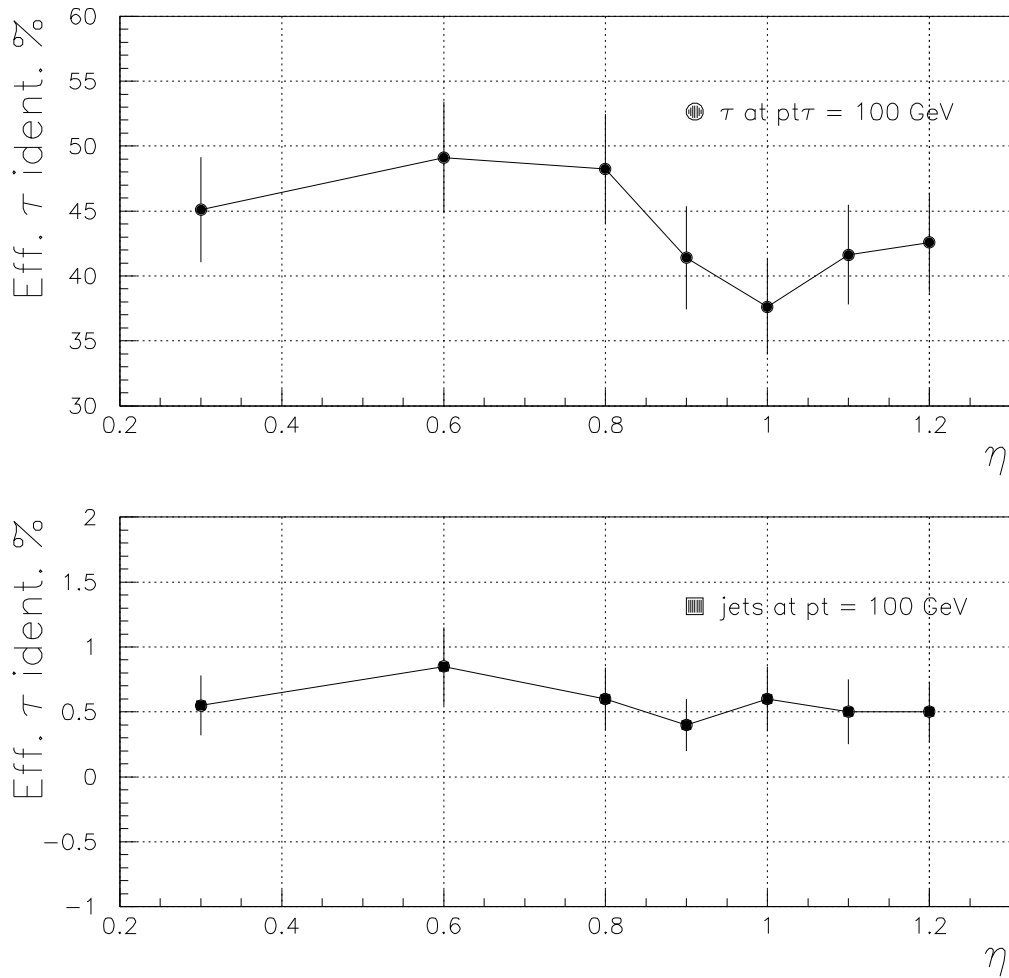


Figure 25: τ -identification efficiencies for isolated τ 's and jets in the crack region 0.7-1.2 between the TILE and the TIXE calorimeter.

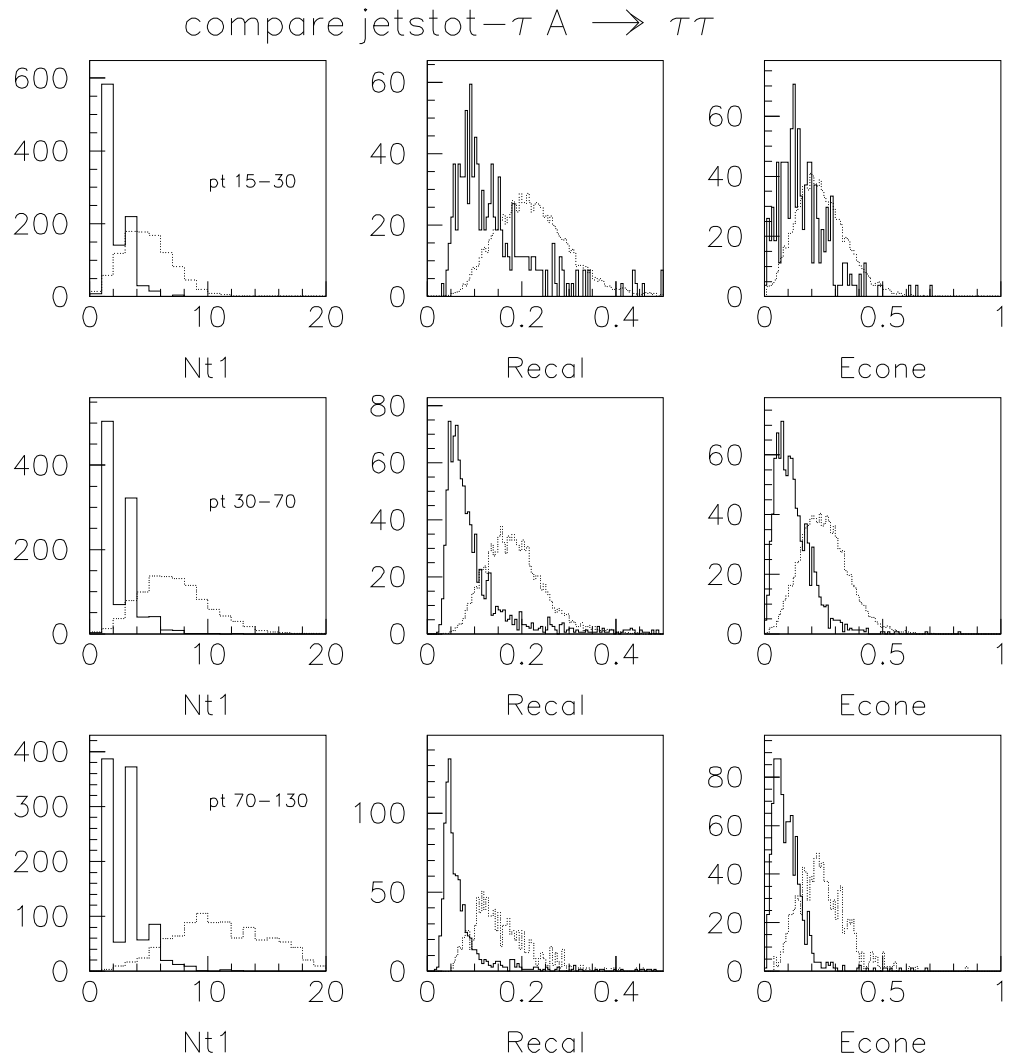


Figure 26: τ -jets (full line) and jets comparison for τ -veto

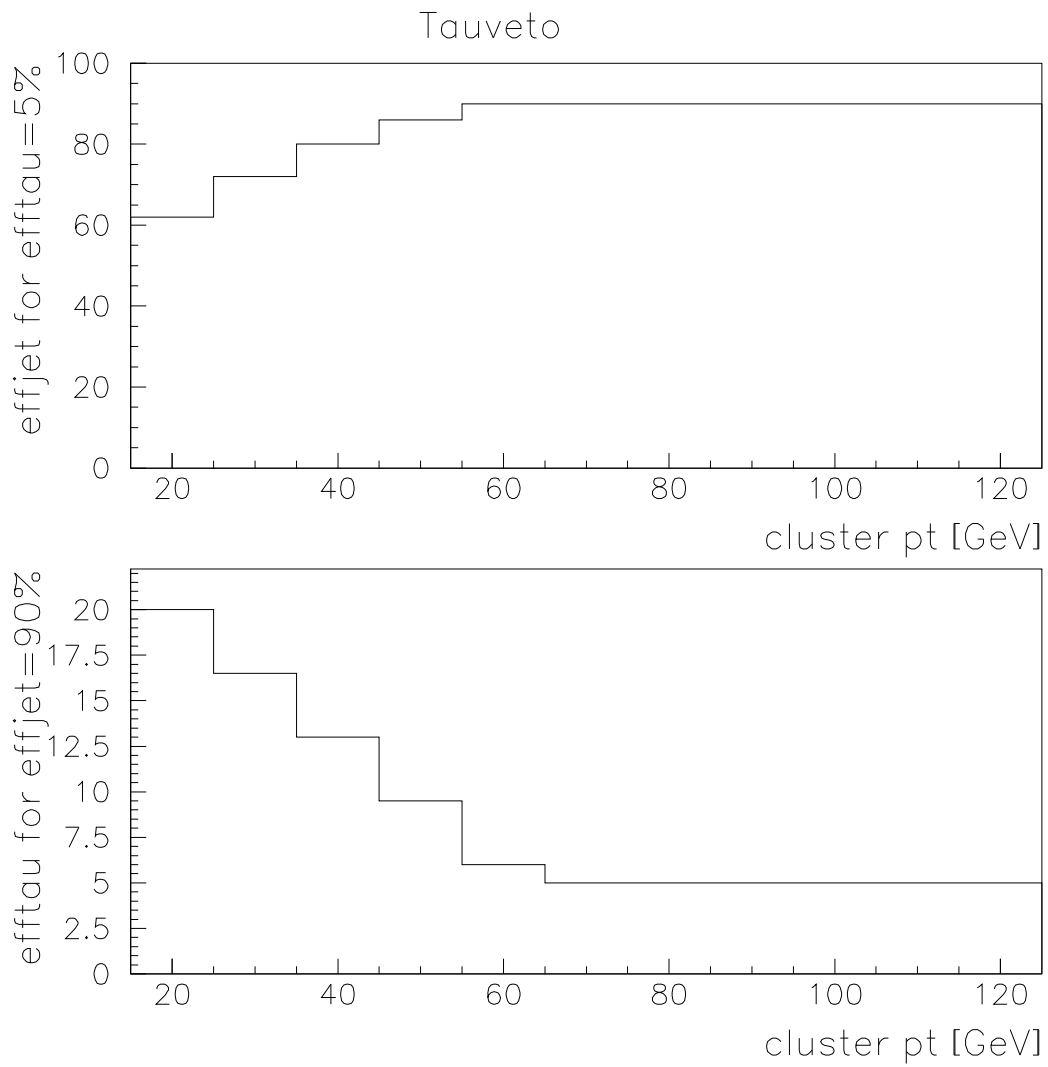


Figure 27: jet-efficiency vs $p_T^{cluster}$ for τ -efficiency fixed to 5%; τ -efficiency vs $p_T^{cluster}$ for jet-efficiency fixed to 90%

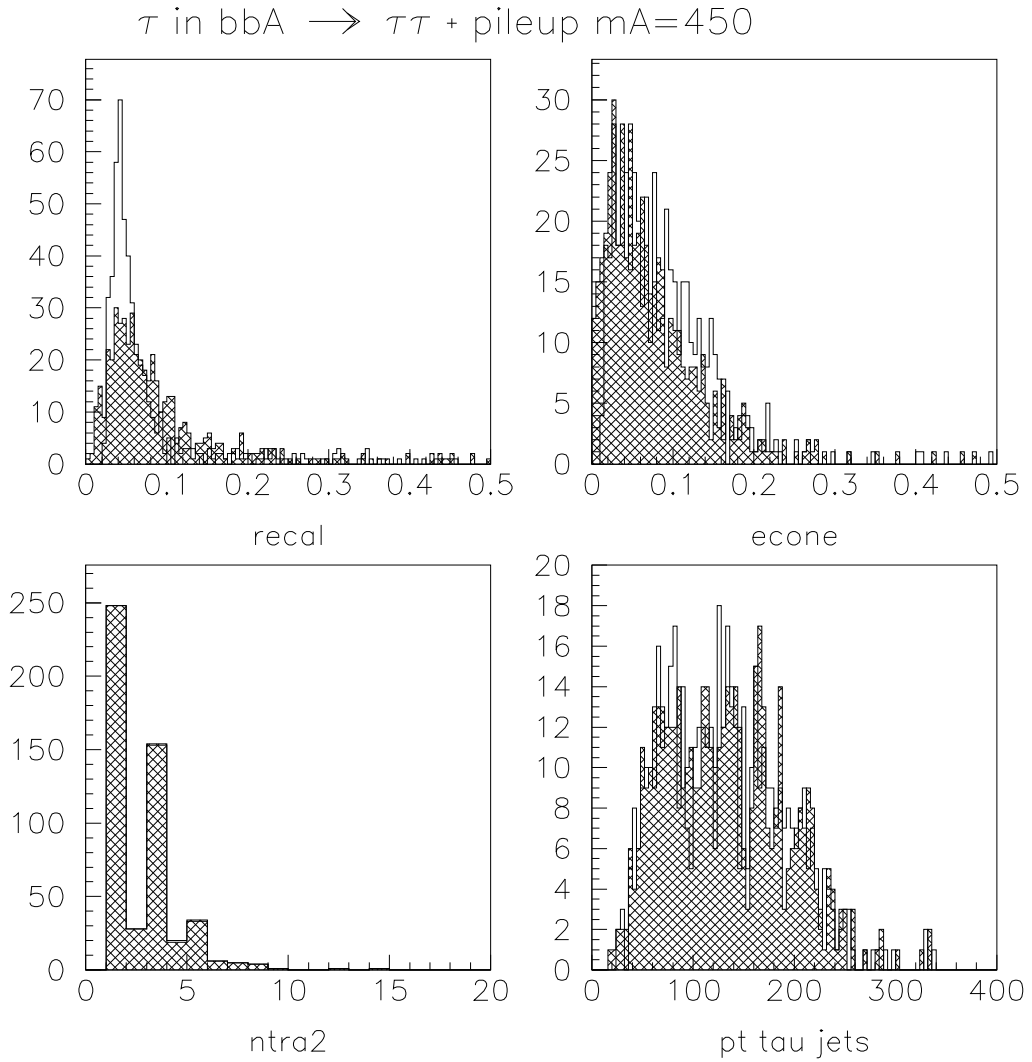


Figure 28: *Distributions of the τ -identification variables and p_T for τ -jets from bbA^0 production + pileup (dashed histograms) superimposed to bbA^0 without pileup*

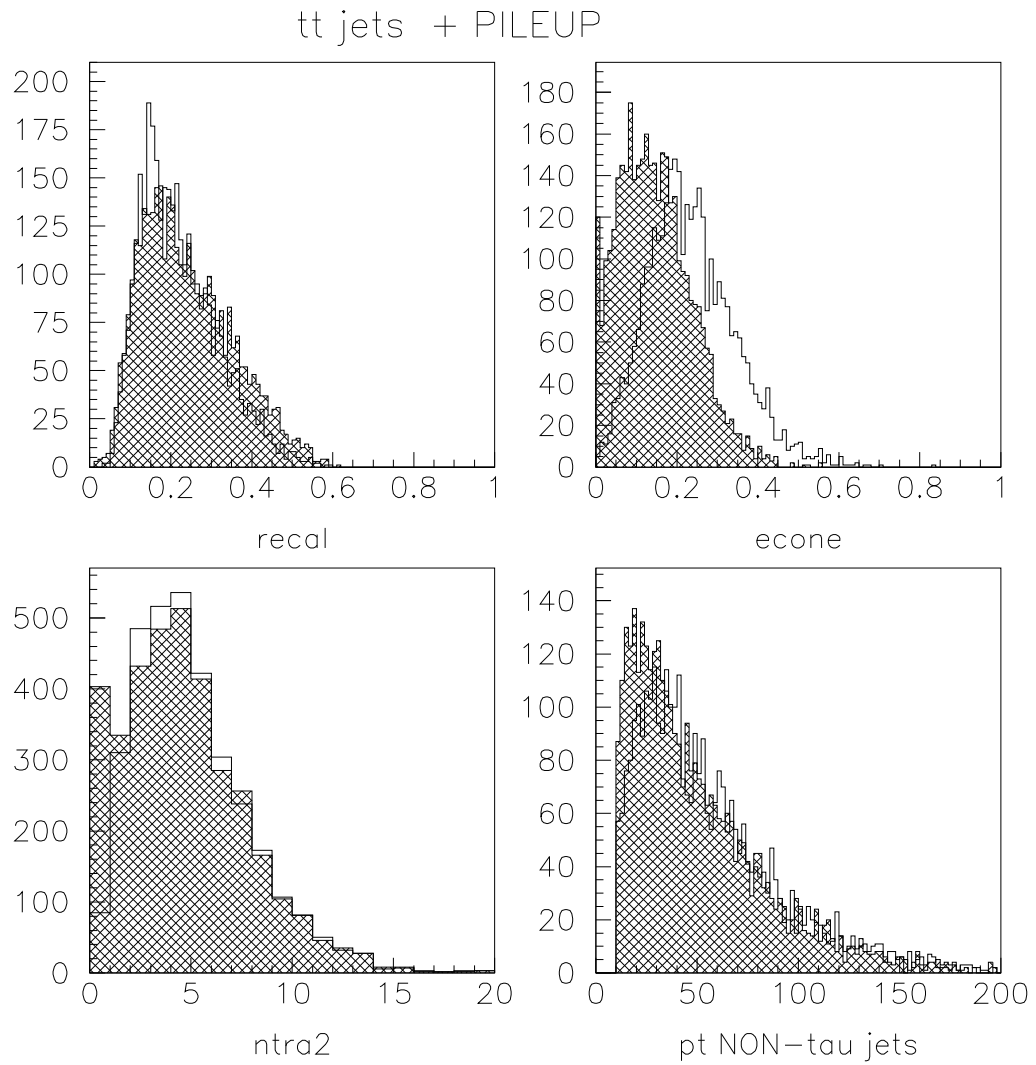


Figure 29: Distributions of the τ -identification variables and p_T for jets from $t\bar{t}$ + pileup (dashed histograms) superimposed to $t\bar{t}$ without pileup